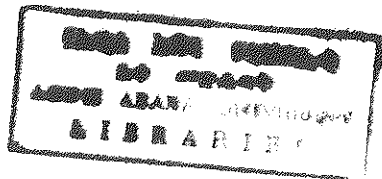


**THEORETICAL STUDIES OF
THE PROPERTIES OF FERROELECTRIC
CERAMIC-POLYMER
COMPOSITE MATERIALS**

SCHOOL OF GRADUATE STUDIES
ADDIS ABABA UNIVERSITY



BY

HUSSEN MOHAMMED

FEBRUARY 1994

*Hus
Che
1994*

ADDIS ABABA UNIVERSITY
SCHOOL OF GRADUATE STUDIES

THEORETICAL STUDIES OF THE PROPERTIES
OF FERROELECTRIC CERAMIC - POLYMER
COMPOSITE MATERIALS

by

Hussain Mohammed

Department of Chemistry
Faculty of Science

Approved by:

Dr. T. J. Sluckin
External examiner

Dr. Haptamu Zewdie
Advisor

Dr. K. Rowberg
Examiner

Dr. L. M. Kachirski
Examiner

Dr. S. S. Kotelinkov
Examiner

Timothy J Sluckin

Habtamu Zewdie

K. Rowberg

L. M. Kachirski

S. S. Kotelinkov

THEORETICAL STUDIES OF
THE PROPERTIES OF FERROELECTRIC
CERAMIC-POLYMER
COMPOSITE MATERIALS

A THESIS

PRESENTED TO

THE SCHOOL OF GRADUATE STUDIES

ADDIS ABABA UNIVERSITY

IN PARTIAL FULFILMENT OF
THE REQUIREMENTS FOR THE DEGREE OF
MASTER OF SCIENCE IN CHEMISTRY

BY

HUSSEN MOHAMMED

FEBRUARY 1994

TO SCIENCE, GOD AND HUMANITY

AND

TO ELIZABETH YOHANNES

Who Doubles Every Triumph,

Halves Every Defeat.

ACKNOWLEDGEMENT

I would like to express my deepest gratitude to my research advisor and instructor Dr. Habtamu Zewdie for identifying the topic of this project, for his consistent supervision and for bringing me the reprints which are not available in the Addis Ababa University libraries.

I am highly indebted to W/t Elizabeth Yohannes who did her best in keeping up the moral and material needs for the successfulness of my work.

I wish to thank the Chemistry Department of Addis Ababa University for sponsoring me to participate in the Graduate Program and all its members for their continued encouragement.

Financial support from DAAD is gratefully acknowledged.

TABLE OF CONTENTS

Title Page	i
Dedication	ii
Acknowledgement	iii
Table of contents	iv
List of Figures	vi
Notations	xi
Abstract	xii
1. Introduction	1
2. Dielectric properties	6
2.1 Introduction	6
2.2 The Series model of dielectricity	11
2.3 The Parallel model of dielectricity	13
2.4 The Spherical particles dispersion theory of dielectricity	14
2.5 The Bruggeman type approximation of dielectricity	18
2.6 The Habtamu Zewdie-F. Brouers theory of dielectricity	20
2.7 The present study of dielectricity	23
3. Elastic properties	25
3.1 Introduction	25
3.2 The Series model of elasticity	29
3.3 The Parallel model of elasticity	31
3.4 The Spherical particles dispersion theory of elasticity	32

3.5	The Habtamu Zewdie-F. Brouers theory of elasticity	33
3.6	The present study of elasticity	37
4.	Piezoelectric Property.....	39
4.1	Introduction.....	39
4.2	Local field coefficients.....	44
4.3	Piezoelectric constants.....	46
5.	Results and Discussions	50
5.1	Proofs of the theoretical predictions	50
5.2	Theoretical predictions on the effect of shape of inclusions	52
5.3	Comparison with experimental data (Volume fraction dependence).....	65
5.3.1	Test on 0-3 connectivity composite	66
5.3.1.1	The dielectric constant	66
5.3.1.2	The elastic constant	68
5.3.1.3	The piezoelectric constant	69
5.3.2	Test on 0-3 connectivity composite with both phases piezoelectrically active	71
5.3.3	Test on 1-1 and 1-3 connectivity composite	73
5.3.3.1	The piezoelectric constant	73
5.3.3.2	The dielectric constant	75
5.4	Comparison with experimental data (Temperature dependence).....	80
6.	Conclusion	88
7.	References	90

- Fig. 2.5.1 Aggregate structure and its equivalent. 18
- Fig. 2.5.2 The BA type model of dielectricity. 18
- Fig. 2.6.1 The four connectivity patterns for a diphasic solid which are experienced in this thesis. Each phase has zero-, one-, two- or three-dimensional connectivity to itself. In the 1-3 connectivity composite, for instance, the shaded phase is three-dimensionally connected and the unshaded phase is one-dimensionally connected. Arrows are used to indicate the connected directions. 21
- Fig. 2.6.2 The HZFB equivalent model of a mixed connectivity composite. In the 1-3 connectivity region the PZT particles are connected in one-dimensions. In the 0-3 connectivity region the PZT particles are zero-dimensionally connected. The polymeric particles are connected in three-dimensions in both cases. 21
- Fig. 2.6.3 Equivalent circuit of the HZFB equivalent model. 22
- Fig. 3.2.1 Schematic depiction of the series model of elasticity. PZT refer to lead zirconate titanate ceramic. 29
- Fig. 3.3.1 Schematic depiction of the parallel model of elasticity. 31
- Fig. 3.4.1 Schematic depiction of the SPDT model of elasticity. c_1 and c_2 stand for the elastic

LIST OF FIGURES

Fig. 1.1	A material (a) before and (b) after poling.	2
Fig. 2.1.1	(a) Schematic representation of a dielectric material whose molecules do not permanent electric dipole moments. (b) When an electric field E is applied to the material.	7
Fig. 2.1.2	(a) Schematic representation of a dielectric material whose molecules have permanent electric dipole moments. The permanence of each dipole is indicated by connecting its two charges with a rigid rod, instead of with a spring. (b) When an electric field E is applied to the material.	8
Fig. 2.1.3	The depolarization field E_d , the applied electric field E , and their vector sum, the internal electric field E_{int} , in a slab of dielectric material. The depolarization field is the electric field produced by the electric dipoles that the molecules of the material constitutes.	9
Fig. 2.2.1	schematic depiction of the series model of dielectricity. PZT refer to lead zirconate titanate ceramic.	11
Fig. 2.3.1	Schematic depiction of the parallel model of dielectricity.	13
Fig. 2.4.1	Schematic depiction of the SPDT model of dielectricity.	15

	constants of the pure components.	33
Fig. 3.5.1	The HZFB equivalent model of a mixed connectivity composite. In the 1-3 connectivity region the PZT particles are connected in one-dimensions. In the 0-3 connectivity region the PZT particles are zero-dimensionally connected. The polymeric particles are connected in three-dimensions in both cases.	34
Fig. 3.5.2	The HZFB model of elasticity.	36
Fig. 5.1	Effect of shape of inclusions on the dielectric constant of a PZT-PVDF composite.	55
Fig. 5.2	Effect of shape of inclusions on the elastic constant of a PZT-PVDF composite.	55
Fig. 5.3	Effect of shape of inclusions on the piezoelectric d constant of a PZT-PVDF composite.	56
Fig. 5.4-5.9	PZT volume fraction and geometric factor dependence of the dielectric, elastic and piezoelectric d constants of a PZT-PVDF composite.	59
Fig. 5.10	PZT volume fraction dependence of the dielectric constant of a PZT-PVDF composite. Comparison of the theoretical predictions and the spherical particle dispersion theory (SPDT) with experimental data.	77
Fig. 5.11	PZT volume fraction dependence of the elastic constant of a PZT-PVDF composite. Comparison of the	

theoretical predictions and the spherical particles dispersion theory(SPDT) with experimental data. 77

Fig. 5.12 PZT volume fraction dependence of the piezoelectric d constant of a PZT-PVDF composite. Comparison of the theoretical predictions and the spherical particles dispersion theory(SPDT) with experimental data. 78

Fig. 5.13 PZT volume fraction dependence of the piezoelectric d constant of a PZT-EPOXY RESIN composite. Comparison of the theoretical predictions and the spherical particles dispersion theory(SPDT) with experimental data. 78

Fig. 5.14 PZT volume fraction dependence of the piezoelectric d constant of a PZT-[VDF-TRFE] composite. Comparison of the theoretical predictions and the spherical particles dispersion theory(SPDT) with experimental data. 79

Fig. 5.15 PZT volume fraction dependence of the dielectric constant of a PZT-EPOXY RESIN composite. Comparison of the theoretical predictions and the spherical particles dispersion theory(SPDT) with experimental data. 79

x

Fig. 5.16-5.21 Temperature dependence of the dielectric, elastic and piezoelectric d constants of a PZT-EPOXY RESIN composite. Comparison of the theoretical predictions and the spherical particles dispersion theory (SPDT) with experimental data.

NOTATION

x, y, z	Rectangular coordinates.
T_{xx}, T_{yy}, T_{zz}	Normal components of stress parallel to $x, y,$ and z axes.
T_{xy}, T_{xz}, T_{yz}	Shearing components in rectangular coordinates.
S_{xx}, S_{yy}, S_{zz}	Normal components of strain parallel to $x, y,$ and z axes.
S_{xy}, S_{xz}, S_{yz}	Shearing strain components in rectangular coordinates.
D	Dielectric displacement.
E	Electric field.
P	Electric polarization.
P_s	Spontaneous polarization.
ϵ_r	Relative permittivity
c	Elastic constant.
S	Strain.
ϵ_0	Permittivity of free space.
n	Geometric factor.
f	PZT Volume fraction.
d, e, g, h	Piezoelectric coupling constants.
L_E, L_D, L_S, L_T	Local field coefficients
PZT	Lead zirconate titanate.
PVDF	Polyvinylidene fluoride.

ABSTRACT

The existing theories which are used to interpret experimental data on the dielectric, elastic and piezoelectric properties of composite materials are summarized. An effective medium theory which treats both components symmetrically has been investigated to show that the geometric factors are important parameters which could take care of both the effects of shape of inclusions and the concept of connectivity, and to demonstrate that the shape of inclusions greatly affect the dielectric, elastic and piezoelectric properties of composite materials.

The properties of composite materials are studied as a function of the PZT volume fraction and the geometric factors and showed that the geometric factor of the component with low volume fraction are more effective and the piezoelectric property of composite materials depend more on the geometric factors for the dielectric constant than on those of the elastic constant.

The theoretical predictions are generalized to study the temperature dependence of the properties of the composite materials.

New expressions for the piezoelectric constants of composite materials are derived and used to study their volume fraction, shape of inclusions and temperature dependence.

Finally, the theoretical predictions are tested with experimental data on a variety of composite materials.

1. INTRODUCTION

Piezo is derived from the greek word meaning 'to press', and piezoelectricity is the creation of an electric charge by an applied stress. It was discovered by J. and P. Curie in 1880. It occurs only in insulating materials and is manifested by the appearance of charges on the surfaces of crystals when they are mechanically deformed.

It is easy to see the nature of the basic molecular mechanisms involved. The application of stress has the effect of separating the centre of gravity of the positive charges from that of the negative charges, producing a dipole moment. This effect can thus occur only in those crystals not having a centre of symmetry, since, for a centro-symmetrical crystal, no combination of uniform stresses will produce the necessary separation of the centres of gravity of the charges. But, today it is also possible to give the polarity needed to impart piezoelectric properties to originally isotropic polycrystalline materials, more or less permanently, by a temporary application of a strong electric field. The process is called poling.

Poling is carried out by applying a strong electric field to the electroded material for a certain period of time at a certain temperature^{1,2}. The figure below shows the dipole moments of a material before and after poling.



Fig. 1.1 A material (a) before and (b) after poling.

The above description makes it clear that the converse piezoelectric effect must exist. When an electric field is applied to a piezoelectric material it will strain mechanically. There is a one-to-one correspondence between the piezoelectric direct effect and its converse in that materials for which strain produces an electric field across them will strain when an electric field is applied.

The creation of useful piezoelectric by treatment of a polycrystalline material depends on ferroelectricity. Ferroelectricity refers to the presence of spontaneous electric moment in a material which can be changed in its orientation between two or more distinct directions by applying an external electric field.

Piezoelectricity is revealed in a composite system of polymers and ferroelectric ceramics if the system is subjected to a high electric field. This causes orientation of dipoles in the composites. As a result, the composites show an electrical response due to a mechanical excitation and a mechanical response due to an electrical excitation²⁻⁶. There has been theoretical investigation of several composite systems, those consisting a

continuous polymer medium and lead zirconate titanate (PZT) ceramic inclusions and those consisting of a continuous PZT ceramic medium and impregnants of polymers⁵⁻⁹. Among those composite systems, those with a continuous polymer medium and PZT ceramic inclusions are very useful because of their plasticity. Such composite systems are easy to mould into various shapes, such as a thin film and thus are useful for technical applications as flexible and filmy transducers with piezoelectric activities⁴⁻⁶.

Theoretical investigations on binary systems have been performed with regard to the piezoelectric constants, the dielectric constant, and the elastic constant^{5,7-9,10}. Piezoelectric, dielectric and elastic properties of ceramic-polymer composite materials are affected by several factors among which are composition, shape, connectivity, properties of the individual components, temperature of measurement^{2,5,11}. In some materials not only are the properties of the separate phases modified, but composites may exhibit completely new couplings not found in the separate phases¹².

One of the inherent problems in composite systems has been in predicting their macroscopic properties using the properties of the constituents. Spherical particle dispersion theory (SPDT)¹³⁻¹⁴ is commonly used to interpret experimental data of composite materials^{5,5,15-17}.

There has been theoretical investigation on the effect of shape of inclusions on the composite dielectric^{4,18,19}, elastic⁴, and piezoelectric d constant⁴ via permittivity. The elastic local

field also depends on the shape of inclusions and affects all the piezoelectric coupling constants²⁰. As the composition of the composite materials change, the role of inclusion and host interchanges. This makes it necessary to consider the shape of the matrix in developing a theory of composite materials.

In this work we will investigate an effective medium theory, which treats both components symmetrically, to study the effects of the shape of inclusions and of connectivity on the properties of composite materials. Connectivity refers to the number of dimensions in which each component phase is self connected between the limiting surfaces of the composite.

In this work we shall:

- (i) Summarize the existing theories which are used to interpret experimental data on the dielectric, elastic, and piezoelectric properties of ceramic-polymer composite materials,
- (ii) Search the literature for data on a variety of composite materials to test the existing theories,
- (iii) Extend the theories to the study of the temperature dependence of the properties of composite materials, and
- (iv) Study the effect of shape of inclusions on the dielectric, elastic, and piezoelectric properties of composite materials.

Chapter 2 is devoted to the dielectric properties of composite materials. The existing theories which are used to interpret experimental data on the dielectric property of composite materials will be summarized. The present study of dielectric properties is given in the end of this chapter.

Chapter 3 is devoted to the elastic properties of composite materials. The existing theories which are used to interpret experimental data on the elastic property of composite materials will be summarized. In the end of this chapter, the present study of elastic properties is given.

Chapter 4 is devoted to the piezoelectric properties of composite materials. New expressions for the local field coefficients and the piezoelectric constants will be derived.

And in chapter 5, the theoretical predictions will be tested with experimental data.

Some brief conclusions are given in chapter 6.

2. DIELECTRIC PROPERTIES

2.1 INTRODUCTION

An insulating substance is called a dielectric. Nearly all practical capacitors are constructed with dielectrics between their electrodes. The principal reason is that the presence of a dielectric increases the capacitance. To understand why, we must understand what happens when an external electric field is applied to a dielectric.

When a dielectric substance is subjected to an external electric field E , electric forces are exerted on the positively and negatively charged particles which comprise the substance. The particles of opposite charge tend to move in opposite directions because the forces exerted on them are oppositely directed. But a dielectric, being an insulator, is a substance in which charged particles are not free to move indefinitely. In describing the motion that does occur, two important cases are to be distinguished.

In the first case there are no permanent electric dipoles in the dielectric substance. That is, there are no dipoles in the absence of the electric field. This means that for each molecule of the dielectric the average location of the negative charge (on the electrons) coincides with the average location of the positive charge (on the nuclei) when there is no applied electric field. When an electric field E is applied to the dielectric from the outside, it induces electric dipoles—called induced

electric dipoles-inside the dielectric. The applied electric field does this by "stretching" each of the molecules so that the average location of the negative charge is displaced from the average location of its positive charge. Figure 2.1.1 illustrates the process, picturing each molecule as a positive and negative charge of equal magnitude whose centres are joined by a spring that represents the attractive forces they exert on

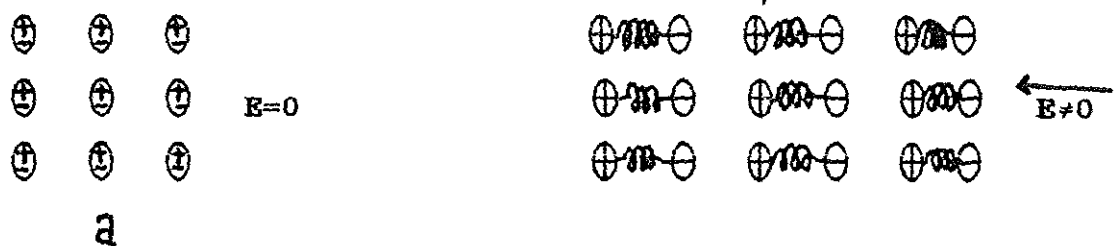


Fig. 2.1.1 (a) Schematic representation of a dielectric material whose molecules do not have permanent electric dipole moments. (b) When an electric field E is applied to the material.

each other. When $E=0$, each spring has zero length and the charges overlap completely. The larger the magnitude of E , the greater is the extension of each spring. Since each induced electric dipole has an electric dipole moment μ of magnitude proportional to the separation of its two charges, the electric dipole moment magnitude increases with increasing the magnitude of the applied electric field. In fact, experiment shows that the magnitude of μ increases in direct proportion to the magnitude of E --provided the applied electric field is not too large (to avoid the destructive electrical breakdown). As for direction, each induced electric dipole moment vector μ , being directed from the negative to the positive charge, is in the direction of the applied electric field vector E .

In the second case, there are permanent electric dipoles in the dielectric substance. For most such substances, in the absence of an applied electric field E these electric dipoles are randomly oriented because of thermal agitation. When the electric field is applied, the equal and opposite forces it exerts on the two charges of each dipole produces torque on the dipole. As indicated schematically in Figure 2.1.2, these torques cause the dipoles to rotate so that their electric dipole moments come into partial alignment with the applied electric field E .

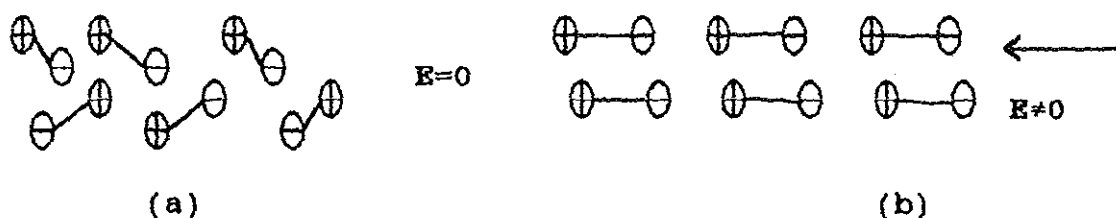


Fig. 2.1.2 (a) Schematic representation of a dielectric material whose molecules have permanent electric dipole moments. The permanence of each dipole is indicated by connecting its two charges with a rigid rod, instead of with a spring. (b) When an electric field E is applied to the material.

Experiment shows that if the applied electric field E is not too large, the average value of the components of μ along the direction of E --a measure of the degree of alignment--is proportional to the magnitude of E .

The following figure (Fig. 2.1.3) shows schematically the macroscopic effect of these microscopic processes. For simplicity, a rectangular slab of dielectric is pictured, whose faces are perpendicular to the direction of a uniform electric field E applied from outside the dielectric. Within the body of the dielectric, electric dipole moments develop--and/or rotate if they are already present--in such a way that on the average the

electric dipole moment vectors are parallel to the applied field vector.

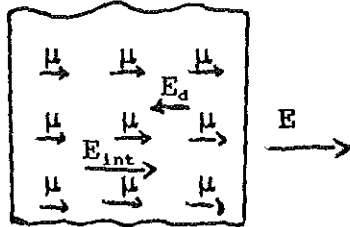


Fig. 2.1.3 The depolarization field E_d , the applied electric field E , and their vector sum, the internal electric field E_{int} , in a slab of dielectric material. The depolarization field is the electric field produced by the electric dipoles that the molecules of the material constitutes.

The electric field E_d of an electric dipole is strongest in the region between the two charges, and in this region E_d is antiparallel to the electric dipole moment μ . But μ is parallel to the electric field E acting on the electric dipole. Hence in the region where E_d is most important because it has the largest magnitude, on the average it has a direction opposite to that of E . This means that as the magnitudes of the electric dipole moments increase--and/or their directions increase the degree of alignment--under the influence of an applied electric field E of increasing magnitude, there comes in to existence a macroscopic, oppositely directed electric field E_d of increasing magnitude resulting from the increasing alignment of the microscopic dipoles. The electric field E_d is called the depolarization field. Since the macroscopic electric dipole moment along the direction of the applied electric field has an average value proportional to the magnitude of the applied field, the magnitude of the depolarization field is also proportional to that of the applied field.

The actual electric field in the interior of the dielectric, E_{int} , is the vector sum of the applied and depolarization fields:

$$E_{int} = E + E_d \quad (2.1.1)$$

Since E and E_d are oppositely directed, the terms in this sum tend to cancel. Thus E_{int} always has a smaller magnitude than E . Also, its magnitude E_{int} is proportional to the magnitude E of the applied electric field since both terms on the right side of equation 2.1.1 have magnitudes proportional to E . This proportional relation between the magnitude of the internal electric field in a dielectric material and the magnitude of the external electric field applied to it is most conveniently stated in terms of the equation

$$\epsilon \equiv E/E_{int} \quad (2.1.2)$$

The quantity ϵ defined in this equation is a constant called the dielectric constant. The value of ϵ is always greater than 1 for any dielectric substance, since E_{int} is always less than E . For vacuum, its value is exactly 1. For a conducting substance the value is $\epsilon = \infty$, because the equilibrium value of E_{int} is always zero in a conductor.

In anisotropic dielectric media the relation between the dielectric displacement D and the electric field E is not a simple proportionality. The most general form of such a relation is

$$D_i = D_{0i} + \epsilon_{ik} E_k \quad (2.1.3)$$

where D_0 is a constant vector, and the quantities ϵ_{ik} form a tensor of rank two, called the dielectric permeability tensor (or simply the dielectric tensor). The inhomogeneous term D_0 in equation 2.1.3 does not however appear for all materials. For isotropic

dielectric materials, the linear relation between the electric displacement D and the electric field E is a simple proportionality:

$$D = \epsilon E \quad (2.1.4)$$

In isotropic dielectric materials, the vectors D and E must be in the same direction. In all our studies we have used this simple relation between D and E .

In sections 2.2-2.6 the existing theories which are used to interpret experimental data on the dielectric property of composite materials will be summarized^{18,20,22-26}. They are in the order of increasing complexity, the series model, the parallel model, the spherical particles dispersion theory (SPDT)¹⁸, the Bruggeman type approximation¹⁸ and the Habtamu Zewdie-F. Brouers theory²⁰. And in section 2.7 our work will be presented. These theories involve calculating the effective dielectric constant of a composite material (ceramic + polymer).

2.2 THE SERIES MODEL OF DIELECTRICITY

Here we have an inhomogeneous macroscopic media where the grain size is practically less than the cluster size. The series model is one of the two extreme models expressing a two phase system. In the series model, shown in Figure 2.2.1, the two phases are stacked along the thickness.

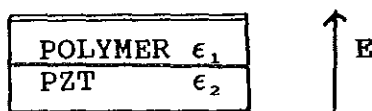


Fig. 2.2.1 schematic depiction of the series model of dielectricity. PZT refer to lead zirconate titanate ceramic.

We assign the polymer phase as phase 1 and the lead zirconate titanate (PZT) phase as phase 2 and distinguish variables and physical constants of respective phases by using suffices 1 and 2. Those with out suffices refer to the whole system. The dielectric equations with respect to phases 1 and 2 are given by,

$$D_1 = \epsilon_1 E_1 \quad (2.2.1)$$

$$D_2 = \epsilon_2 E_2 \quad (2.2.2)$$

where D is dielectric displacement, E is the electric field and ϵ is permittivity.

In the series model, the electric fields in the respective phases are usually unequal and satisfy the following relation,

$$E = (1-f)E_1 + fE_2 \quad (2.2.3)$$

where f is the volume fraction of phase 2. The dielectric displacement is continuous along the thickness. Thus we have

$$D = D_1 = D_2. \quad (2.2.4)$$

Using equations 2.1.4, 2.2.1 and 2.2.2 we can write eq. 2.2.3 as

$$D/\epsilon = (1-f)D_1/\epsilon_1 + fD_2/\epsilon_2. \quad (2.2.5)$$

And using eq. 2.2.4 in 2.2.5, we get

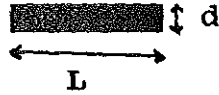
$$1/\epsilon = (1-f)/\epsilon_1 + f/\epsilon_2. \quad (2.2.6)$$

Rearranging, we get

$$\epsilon = \epsilon_1 \epsilon_2 / ((1-f)\epsilon_2 + f\epsilon_1) \quad (2.2.7)$$

This is an expression for the effective dielectric constant ϵ of a two phase system, where the two phases are stacked along the thickness, in terms of the dielectric constants of the two

components (ϵ_1 and ϵ_2) and the concentrations of the two components (f and $1-f$). This model is good if the correlation length ζ gives the average size of cluster, i.e., $d \ll \zeta \ll L$.



2.3 THE PARALLEL MODEL OF DIELECTRICITY

The two extreme models expressing a two phase system are the series and the parallel models. In the parallel model, shown in Figure 2.3.1, the two phases are connected side by side.



Fig. 2.3.1 Schematic depiction of the parallel model of dielectricity.

We assign the polymer phase as phase 1 and the lead zirconate titanate (PZT) phase as phase 2 and distinguish variables and physical constants of respective phases by using suffices 1 and 2. Those with out suffices refer to the whole system.

In the parallel model, the internal fields (E_1 and E_2) appearing in respective phases are equal to the applied field E and the dielectric displacements (D_1 and D_2) are additive,

$$E = E_1 = E_2 \quad (2.3.1)$$

and

$$D = (1-f)D_1 + fD_2 \quad (2.3.2)$$

where f is the PZT volume fraction.

Using eqs. 2.1.4, 2.2.1 and 2.2.2 we can write eq. 2.3.2 as

$$\epsilon E = (1-f)\epsilon_1 E_1 + f\epsilon_2 E_2 \quad (2.3.3)$$

And using eqs. 2.3.1 and 2.3.3, we get

$$\epsilon = (1-f)\epsilon_1 + f\epsilon_2. \quad (2.3.4)$$

This is an expression for the effective dielectric constant ϵ of a two phase system, where the two phases are connected side by side, in terms of the dielectric constants of the pure components (ϵ_1 and ϵ_2) and the concentrations of the two phases (f and $(1-f)$). This model is good if $d \gg \zeta \gg L$, where ζ is the correlation length. In practice neither assumption is good and $\zeta \ll d \approx L$. This is one of the disadvantages of the parallel and the series models.

2.4 THE SPHERICAL PARTICLES DISPERSION THEORY (SPDT) OF DIELECTRICITY

In sections 2.2 and 2.3 we have seen composite materials where the two phases are either stacked along the thickness (the series model) or connected side by side (the parallel model). There is a third case when the mixture of the polymer and lead zirconate titanate (PZT) powder makes a two phase system, where PZT particles are dispersed in a continuous polymer matrix, or vice versa. This two phase dispersion system has a combined character of the series and the parallel models. Usually such systems are treated using the spherical particles dispersion theory (SPDT)^{13-14,18,31}.

In this section the spherical particles dispersion theory of dielectricity will be summarized. SPDT is used for a separated grain structure, where the PZT and polymer exhibit an asymmetric topology consisting of either PZT inclusions in a polymer matrix

or polymer inclusions in a PZT matrix.

The SPDT model, shown in Figure 2.4.1, consists of a random unit of a coated sphere, for instance an internal sphere of component 2 surrounded by component 1. This system is subjected to an as yet unknown, effective medium which is determined to be such that the resulting extra perturbation vanishes on the average over all possibilities of the random unit.

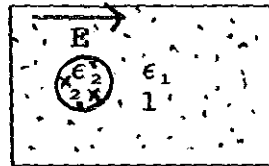


Fig. 2.4.1 Schematic depiction of the SPDT model of dielectricity.

The electric field in phase 1 E_1 is equal to the applied electric field E . To have an expression for the effective dielectric constant of the two phase system first we have to express the electric field in phase 2 E_2 in terms of E .

We denote the dielectric constant of phase 2 by ϵ_2 and that of component by ϵ_1 . We take the origin of spherical coordinates at the centre of the sphere, and the direction of E as the polar axis, and seek the field potential outside the sphere.

We write the potential in the form $\phi = \phi_0 + \phi_1$, where $\phi_0 = E \cdot r$ is the potential of the external field and ϕ_1 is the required change in potential due to the sphere. By symmetry, the function ϕ_1 can depend only on the constant vector E . The only such solution of Laplace's equation which vanishes at infinity is

$$\phi_1 = \text{constant} \times E \cdot \text{grad}(1/r) = \text{constant} \times E \cdot r / r^3 = E \cdot r (A/r^3)$$

Inside the sphere, we seek the field potential to the form $\Phi_2 = -BE \cdot r$, the only function which satisfies Laplace's equation, remains finite at the centre of the sphere, and depends only on the constant vector E .

The constants A and B are determined by the boundary conditions on the surface of the sphere. It may be seen at once, however, that the field in the sphere $E_2 = BE$ is uniform and differs only in magnitude from the applied field E .

The boundary condition of continuity of potential gives $E_2 = E(1-A/R^3)$, where R is the radius of the sphere, and the condition of continuity of the normal component of the electric displacement D gives $D_2 = \epsilon_1 E(1+2A/R^3)$. Eliminating A from these two equations, we obtain

$$(D_2 + 2\epsilon_1 E_2) = 3\epsilon_1 E \quad (2.4.1)$$

or, substituting $D_2 = \epsilon_2 E_2$,

$$E_2 = 3\epsilon_1 E / (2\epsilon_1 + \epsilon_2) \quad (2.4.2)$$

This equation was modified by Landau and Lifshitz²¹ for different shape of inclusions by including a shape parameter in the direction of the field, n , as

$$E_2 = \epsilon_1 E / ((1-n)\epsilon_1 + n\epsilon_2). \quad (2.4.3)$$

The shape parameter n has values ranging from zero to unity for different average shapes of inclusions. For example, if the inclusions have on the average prolate shape it takes values zero. If the inclusions have on the average a spherical shape it takes the value $1/3$. It has the value unity for an oblate shaped inclusions and intermediate values for intermediate average shape

of inclusions.

We know that the electric field in phase 2 (eq. 2.1.1) is given by,

$$\mathbf{E}_2 = \mathbf{E} + \mathbf{E}_2^{\text{dep}} \quad (2.4.4)$$

where $\mathbf{E}_2^{\text{dep}}$ is the depolarization field in phase 2.

Comparing eqs. 2.4.3 and 2.4.4 gives

$$\mathbf{E}_2^{\text{dep}} = -n(\epsilon_2 - \epsilon_1)\mathbf{E}/((1-n)\epsilon_1 + n\epsilon_2) \quad (2.4.5)$$

Now that we have an expression for \mathbf{E}_2 in terms of \mathbf{E} we will try to get an expression for the effective dielectric constant of the two phase system. The two phase spherical dispersion system has a combined character of parallel and series models. Thus we have,

$$\mathbf{E} = (1-f)\mathbf{E}_1 + f\mathbf{E}_2 \quad (2.4.6)$$

and

$$\mathbf{D} = (1-f)\mathbf{D}_1 + f\mathbf{D}_2 \quad (2.4.7)$$

where f is the PZT volume fraction .

Using eqs. 2.1.4, 2.2.1 and 2.2.2 we can write eq. 2.4.7 as

$$\epsilon\mathbf{E} = (1-f)\epsilon_1\mathbf{E}_1 + f\epsilon_2\mathbf{E}_2. \quad (2.4.8)$$

Since $\mathbf{E} = \mathbf{E}_1$, substituting the values of \mathbf{E}_2 (eq. 2.4.2) and \mathbf{E} (eq. 2.4.6) in eq. 2.4.8, and rearranging, we get

$$\epsilon = \epsilon_1(2\epsilon_1 + \epsilon_2 - 2f(\epsilon_1 - \epsilon_2))/(2\epsilon_1 + \epsilon_2 - f(\epsilon_2 - \epsilon_1)) \quad (2.4.9)$$

This is an expression for the effective dielectric constant ϵ of a two phase spherical dispersion system in terms of the dielectric constants of the pure components (ϵ_1 and ϵ_2) and the concentrations of the two components (f and $(1-f)$).

2.5 THE BRUGGEMAN TYPE APPROXIMATION OF DIELECTRICITY.

In section 2.4 we have seen the spherical particles dispersion theory being used to calculate the effective dielectric constant of a two phase dispersion system. The other approximation commonly used is the Bruggeman type approximation(BA)^{18,30}.

In this section the Brouers¹⁸ version of the BA type approximation of dielectricity will be summarized. The BA type approximation is used for an aggregate structure where the polymer and lead zirconate titanate(PZT) grains are interdispersed and topologically equivalent. The heterogeneous structure is assumed to be a homogeneously dispersed system.

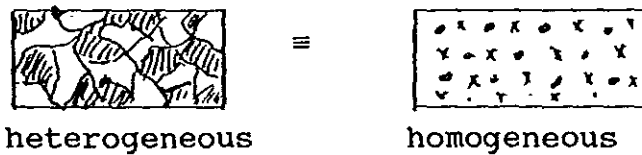


Fig. 2.5.1 Aggregate structure and its equivalent.

The BA type model, shown in Figure 2.5.2, consists of a random unit of both components(1 and 2) embedded in an effective medium. The two components are treated symmetrically and the role of inclusion and host interchanges as the composition of the composite is changed. This is an advantage over the SPDT model where one component is always solute and the other always solvent.

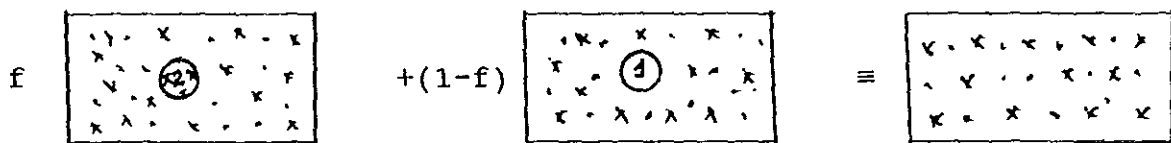


Fig. 2.5.2 The BA type model of dielectricity.

The electric fields inside the inclusions of the two components are given by

$$\mathbf{E}_1 = \mathbf{E} + \mathbf{E}_1^{\text{dep}} \text{ and } \mathbf{E}_2 = \mathbf{E} + \mathbf{E}_2^{\text{dep}}. \quad (2.5.1)$$

Using eq. 2.4.5 the depolarization fields of the two components are

$$\mathbf{E}_2^{\text{dep}} = -n_2(\epsilon_2 - \epsilon)\mathbf{E}/((1-n_2)\epsilon + n_2\epsilon_2) \quad (2.5.2)$$

and

$$\mathbf{E}_1^{\text{dep}} = -n_1(\epsilon_1 - \epsilon)\mathbf{E}/((1-n_1)\epsilon + n_1\epsilon_1). \quad (2.5.3)$$

The two phase dispersion system has a combined character of the series and parallel models. Thus, both the electric fields and the dielectric displacements of the two phases are additive.

$$\mathbf{E} = (1-f)\mathbf{E}_1 + f\mathbf{E}_2 \quad (2.5.4)$$

and

$$\mathbf{D} = (1-f)\mathbf{D}_1 + f\mathbf{D}_2 \quad (2.5.5)$$

where f is the PZT volume fraction. This is a self consistent field theory.

Substituting for \mathbf{E}_1 and \mathbf{E}_2 in eq. 2.5.4, we get

$$\mathbf{E} = f(\mathbf{E} + \mathbf{E}_2^{\text{dep}}) + (1-f)(\mathbf{E} + \mathbf{E}_1^{\text{dep}}). \quad (2.5.6)$$

Using the values of $\mathbf{E}_1^{\text{dep}}$ and $\mathbf{E}_2^{\text{dep}}$ from eqs. 2.5.2. and 2.5.3, and rearranging, we obtain

$$f\epsilon/((1-n_2)\epsilon + n_2\epsilon_2) + (1-f)\epsilon/((1-n_1)\epsilon + n_1\epsilon_1) = 1 \quad (2.5.7)$$

This is an expression for the effective dielectric constant ϵ of a two phase system in terms of the respective constants of the pure components (ϵ_1 and ϵ_2), the PZT volume fraction f and the geometric factors of the two phases (n_1 and n_2).

2.6 THE HABTAMU ZEWDIE-F. BROUERS(HZFB) THEORY OF DIELECTRICITY

In sections 2.2, 2.3 and 2.4 we have seen how the effective dielectric constant of a two phase system is evaluated from the respective constants of the pure components and their concentrations. And in section 2.5 we have an expression which includes the effect of shape of inclusions. In this section the HZFB²⁰ theory of dielectricity will be summarized. In the HZFB theory, the concept of connectivity is incorporated in addition to all the factors involved in the previous theories.

Connectivity refers to the number of dimensions in which each component phase is self connected between the limiting surfaces of the composite. the concept of connectivity plays an important role in understanding the behaviour of composite materials. Connectivity is a key feature in property development in multiphase solids since physical properties can change by many orders of magnitude depending on the manner in which connections are made. Each phase in a composite may be self-connected in zero, one, two or three dimensions. It is natural to confine attention to the perpendicular axes because all property tensor are referred to such systems. If we limit ourselves to diphasic composites, there are ten connectivities: 0-0, 0-1, 0-2, 0-3, 1-1, 1-2, 1-3, 2-2, 2-3 and 3-3. The connectivity patterns which we will encounter in this thesis are illustrated in Figure 2.6.1 using a cube as the basic building block. A 1-1 connectivity

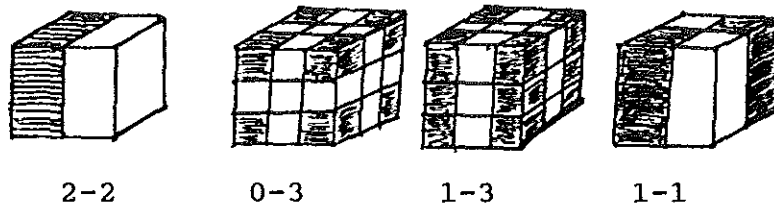


Fig. 2.6.1 These are the four connectivity patterns for a diphasic solid which are encountered in this thesis. Each phase has zero-, one-, two- or three-dimensional connectivity to itself. In the 1-3 connectivity composite, for instance, the shaded phase is three-dimensionally connected and the unshaded phase is one-dimensionally connected. Arrows are used to indicate the connected directions.

pattern, for example, has both phases self-connected in one dimensional chains or fibres. Connectivity patterns for more than two phases are basically similar to the diphasic patterns, but far more numerous. There are 20 three-phase patterns and 35 four-phase patterns compared to the ten two-phase patterns. For n phases the number of connectivity patterns is $(n + 3)!/(3!n!)$. Tri-phasic connectivity patterns are important when electrode patterns are incorporated in the diphasic ceramic structures.

The HZFB model, shown in Figure 2.6.2, more approximates real system by treating it as a mixed connectivity composite.

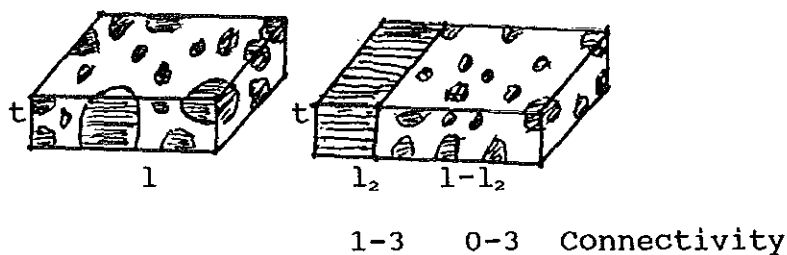


Fig. 2.6.2 The HZFB equivalent model of a mixed connectivity composite. In the 1-3 connectivity region the PZT particles are connected in one-dimensions. In the 0-3 connectivity region the PZT particles are zero-dimensionally connected. The polymeric particles are connected in three-dimensions in both cases.

The HZFB model considers the polarization of a composite with mixed connectivity as a sum of contributions from the 0-3 and 1-3 connectivity volume fractions of the PZT,

$$P_{\text{comp}} = P_{0-3} + P_{1-3} \quad (2.6.1)$$

$$\text{where } P_{0-3} = f_{0-3} L_E P_2 \quad (2.6.2)$$

$$P_{1-3} = f_{1-3} P_2 \quad (2.6.3)$$

P_2 is the PZT polarization, and L_E is the local field coefficient defined by eq. 4.2.2, f_{0-3} and f_{1-3} are the 0-3 and 1-3 connectivity volume fractions of PZT.

The dielectric constant of the 1-3 connectivity region is ϵ_2 . And the effective dielectric constant of the 0-3 connectivity region is calculated using the BA type approximation (see section 2.5) as²⁰

$$\begin{aligned} & f_{0-3} \epsilon_{0-3} / ((1-n_2) \epsilon_{0-3} + n_2 \epsilon_2) + \\ & (1-f_{0-3}) \epsilon_{0-3} / ((1-n_1) \epsilon_{0-3} + n_1 \epsilon_1) = 1. \end{aligned} \quad (2.6.4)$$

The PZT volume fraction of the 1-3 connectivity region f_{1-3} is calculated using Monte Carlo method²⁰. Once the PZT volume fractions of the two connectivity regions are known, the equivalent circuit, shown in Figure 2.6.3, is used to calculate the effective dielectric constant of the composite through the calculation the composite capacitance C_{comp} .

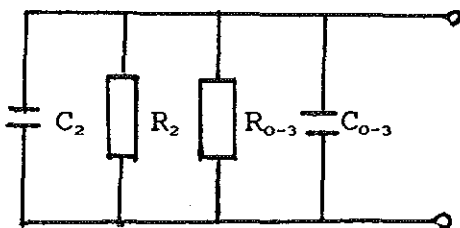


Fig. 2.6.3 Equivalent circuit of the H2FB equivalent model.

The RC parallel elements of the equivalent circuit represents the portion of the composite with 1-3 connectivity and 0-3 connectivity. R_2 and C_2 refer to the resistance and capacitance of the PZT and R_{0-3} and C_{0-3} to that of the remaining

matrix with 0-3 connectivity. The corresponding capacitances are given by

$$C_2 = \epsilon_0 \epsilon_2 A_2 / t, \quad (2.6.5)$$

and

$$C_{0-3} = \epsilon_0 \epsilon_{0-3} A / t, \quad (2.6.6)$$

where ϵ_{0-3} is the effective dielectric constant of the portion with 0-3 connectivity calculated via eq. 2.6.4. The parameters of the model l_2 , l and t , are determined by

$$l_2 t = 1, \quad l_2 l t = f_{1-3}, \quad l(1-l_2)t = 1-f_{1-3}, \quad (2.6.7)$$

$$\text{with } A_2 = l l_2, \quad A = l(1-l_2) \quad (2.6.8)$$

$$\text{and } A_{\text{comp}} = A + A_2 \quad (2.6.9)$$

The total capacitance of the system is given as

$$C_{\text{comp}} = C_2 + C_{0-3}, \quad (2.6.10)$$

from which the total effective dielectric constant is determined as

$$\epsilon_{\text{comp}} = C_{\text{comp}} t / (\epsilon_0 A_{\text{comp}}) \quad (2.6.11)$$

This is an expression for the effective dielectric constant of a two phase system and it includes the effects of the shape of inclusions, connectivity, individual dielectric constants and the concentrations of the two phases.

2.7 PRESENT STUDY OF DIELECTRICITY

In our work we study the dielectric property of composite materials giving emphasis to the effect of shape of inclusions measured by the geometric factor n . To do this we have selected the BA type approximation because its predictions are expected to be good in the whole PZT volume fraction range since both phases

are treated symmetrically in contrast to the SPDT model where one component is always solute and the other is always solvent. The predictions of the SPDT model are expected to be poor in the middle volume fraction range. The BA type approximation is advantageous over the HZFB theory in its simplicity. Can the concept of connectivity be taken care of by the geometric factors in the BA type approximation? This is what we are going to see in chapter 5. To test this theories, we will compare the expressions for the effective dielectric constant of a composite by the SPDT(eq. 2.4.9) and the BA(eq. 2.5.7) with experimental data in section 5.

3. ELASTIC PROPERTIES

3.1 INTRODUCTION

It is well known that some materials are stiffer than others. This means, stated precisely, that if two identical forms are fabricated from different materials, the object made of the stiffer material will distort less than the less stiff material for the same applied force F . This leads us naturally to try to express the stiffness of a material quantitatively, in such a way that it is independent of the form in which the material happens to be fabricated. This is of great practical importance to the engineer, for example, who knows what materials are available and needs to design a structure which will bear a given load.

Other things being equal, the change in length of a bar of material when it is subjected to a given external force is directly proportional to its length. In order to make possible comparisons of samples of material when they are subjected to external forces, in a way which is independent of their length, the strain S is defined to be:

$$S \equiv \Delta l/l. \quad (3.1)$$

The strain S is the change in length of a sample per unit of un distorted length l of the sample. Since strain is a quotient of two lengths, it is a dimensionless number. The value of strain is positive for stretch and negative for compression. In the more general case, suppose that during deformation the points of

a medium undergo a displacement u whose components are denoted by u_x , u_y and u_z . The deformation of the medium is characterized by the symmetrical strain tensor

$$S = \begin{vmatrix} S_{xx} & S_{xy} & S_{xz} \\ S_{xy} & S_{yy} & S_{yz} \\ S_{xz} & S_{yz} & S_{zz} \end{vmatrix} \quad (3.2)$$

whose components are

$$\begin{aligned} S_{xx} &= \partial u_x / \partial x & S_{yy} &= \partial u_y / \partial y & S_{zz} &= \partial u_z / \partial z \\ S_{xy} &= (1/2)(\partial u_x / \partial y + \partial u_y / \partial x) & S_{xz} &= (1/2)(\partial u_x / \partial z + \partial u_z / \partial x) \\ S_{yz} &= (1/2)(\partial u_y / \partial z + \partial u_z / \partial y) \end{aligned} \quad (3.3)$$

Now that we have defined a quantity, strain, which is independent of the length of a sample, we define a quantity which is independent of its thickness. Other things being equal, the stiffness of a rod (its ability to resist stretching) is directly proportional to its cross-sectional area. This is because the applied force may be thought of as divided evenly among the individual members of the imaginary bundle of rods of which the actual rod is made up. In order to make comparisons of samples of material when they are subjected to external force F , in a way which is independent their cross-sectional areas A , the stress T is defined to be:

$$T \equiv F/A \quad (3.4)$$

The quantity T is more precisely called the uniaxial stress, that is the stress along a single axis. It is defined to be the total force applied to an object along that axis, divided by the cross-

$$T_i = c_{ij}S_j \quad (3.7)$$

where $i, j = 1, \dots, 6$. The thirty-six elastic constants are not all independent. We observe that an increment of the strain-energy density, U , is given by

$$dU = T_{xx}dS_{xx} + T_{yy}dS_{yy} + T_{zz}dS_{zz} + T_{yz}dS_{yz} + T_{zx}dS_{zx} + T_{xy}dS_{xy}. \quad (3.8)$$

Since the strain energy may be regarded as a single valued function of the strains, it follows that

$$\partial T_{xx} / \partial S_{yy} = \partial T_{yy} / \partial S_{xx}; \quad (3.9)$$

and hence, from eq.3.6,

$$c_{12} = c_{21}.$$

Similarly, one finds that, in general,

$$c_{ij} = c_{ji}. \quad (3.10)$$

The matrix $\|c\|$ is therefore symmetrical. This symmetry relation reduce the number of independent constants from thirty-six to twenty-one. The elastic constant(c) is analogous to the dielectric constant(ϵ) in that both are medium response functions. For isotropic materials, the number of independent constants reduce to two. They are: the modulus of rigidity G which is the ratio of shear stress to shear strain and the bulk modulus or incompressibility B which is the ratio of the hydrostatic pressure to the dilatation it produces. On the further assumption of incompressibility of the materials we will have only one expression for the elastic constant of materials and the relation between stress T and strain S will simply be

$$T = cS \quad (3.11)$$

In all our studies we have used this simple relation between stress and strain.

In sections 3.2-3.5 the existing theories which are used to interpret experimental data on the elastic property of composite materials will be summarized^{13,20,27,28}. They are in the order of increasing complexity: the series model, the parallel model, the spherical particles dispersion theory(SPDT)¹³ and the Habtamu Zewdie-F. Brouers(HZFB) theory²⁰. And in section 3.6 the present study of elasticity is presented.

3.2 THE SERIES MODEL OF ELASTICITY

The series model is one of the two extreme models which are used to calculate the effective elastic constant of a two phase system. In the series model, shown in Figure 3.2.1, the two phases are stacked along the thickness.

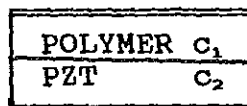


Fig. 3.2.1 schematic depiction of the series model of elasticity. PZT refer to lead zirconate titanate ceramic.

We assign the polymer phase as phase 1 and the lead zirconate titanate(PZT) phase as phase 2 and distinguish variables and physical constants of respective phases by using suffices 1 and 2. Those with out suffices refer to the whole system. The elastic equations with respect to phases 1 and 2 are given by,

$$T_1 = c_1 S_1 \quad (3.2.1)$$

$$T_2 = c_2 S_2 \quad (3.2.2)$$

where T is stress, S is strain and c is the elastic constant.

In the series model, the strains in the respective phases are usually unequal and satisfy the following relation,

$$S = fS_2 + (1-f)S_1 \quad (3.2.3)$$

where f is the volume fraction of phase 2. The stress is continuous along the thickness. Thus we have

$$T = T_1 = T_2. \quad (3.2.4)$$

Using equations 3.1.11, 3.2.1 and 3.2.2 we can write eq. 3.2.3 as

$$T/c = (1-f)T_1/c_1 + fT_2/c_2. \quad (3.2.5)$$

And using eq. 3.2.4 in 3.2.5, we get

$$1/c = (1-f)/c_1 + f/c_2. \quad (3.2.6)$$

Rearranging, we get

$$c = c_1c_2/((1-f)c_2 + fc_1) \quad (3.2.7)$$

This is an expression for the effective elastic constant c of a two phase system, where the two phases are stacked along the thickness, in terms of the elastic constants of the two components (c_1 and c_2) and the concentrations of the two components (f and $1-f$).

2.3 THE PARALLEL MODEL OF ELASTICITY

This is the other extreme model expressing a two phase system. In the parallel model, shown in Figure 3.3.1, the two phases are connected side by side.

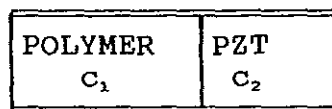


Fig. 3.3.1 Schematic depiction of the parallel model of elasticity.

We assign the polymer phase as phase 1 and the lead zirconate titanate (PZT) phase as phase 2 and distinguish variables and physical constants of respective phases by using suffices 1 and 2. Those without suffices refer to the whole system.

In the parallel model, the internal strains (S_1 and S_2) appearing in respective phases are equal to the applied strain S and the stresses (T_1 and T_2) are additive,

$$S = S_1 = S_2 \quad (3.3.1)$$

and

$$T = (1-f)T_1 + fT_2 \quad (3.3.2)$$

where f is the PZT volume fraction.

Using eqs. 3.1.11, 3.2.1 and 3.2.2 we can write eq. 3.3.2 as

$$cS = (1-f)c_1S_1 + fc_2S_2 \quad (3.3.3)$$

And using eq. 3.3.1 in 3.3.3, we get

$$c = (1-f)c_1 + fc_2 \quad (3.3.4)$$

This is an expression for the effective elastic constant c of a two phase system, where the two phases are connected side by

side, in terms of the elastic constants of the pure components(c_1 and c_2) and the concentrations of the two phases(f and $(1-f)$).

3.4 THE SPHERICAL PARTICLES DISPERSION THEORY(SPDT) OF ELASTICITY

In sections 3.2 and 3.3 we have seen composite materials where the two phases are either stacked along the thickness(the series model) or connected side by side(the parallel model). There is a third case when the mixture of the polymer and lead zirconate titanate(PZT) powder makes a two phase system, where PZT particles are dispersed in a continuous polymer matrix, or vice versa. Similar to the dielectric properties which are discussed in chapter 2, this two phase dispersion system has a combined character of the series and the parallel models. There are two theories which treat such systems. They are the spherical particles dispersion theory(SPDT)¹³ and the Habtamu Zewdie-F. Brouers Theory²⁰.

In this section we will see the spherical particles dispersion theory(SPDT) of elasticity. SPDT is used for a separated grain structure, where the PZT and polymer exhibit an asymmetric topology consisting of either PZT inclusions in a polymer matrix or polymer inclusions in a PZT matrix.

The SPDT model, shown in Figure 3.4.1, consists of a random unit of a coated sphere, for instance an internal sphere of component 2 surrounded by component 1. This system is subjected to an as yet unknown, effective medium which is determined to be

such that the resulting extra perturbation vanishes on the average over all possibilities of the random unit.

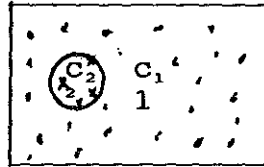


Fig. 3.4.1 Schematic depiction of the SPDT model of elasticity. c_1 and c_2 stand for the elastic constants of the pure components.

The SPDT model effective elastic constant c of a two phase spherical dispersion system has been derived by Chen²² to be

$$c = c_1(3c_1 + 2c_2 - 3f(c_1 - c_2))/(3c_1 + 2c_2 - 2f(c_2 - c_1)) \quad (3.4.1)$$

where c_1 and c_2 are the elastic constants of the pure polymer and PZT phases, respectively and f refers to the PZT volume fraction.

3.5 THE HABTAMU ZEWDIE-F. BROUERS(HZFB) THEORY OF ELASTICITY.

In sections 3.2, 3.3 and 3.4 we have expressions for the effective elastic constant of a two phase system is evaluated from the respective constants and concentrations of the pure components. In this section the HZFB²⁰ theory of elasticity will be summarized. In the HZFB theory, both the concept of connectivity and the effect of shape of inclusions are incorporated in addition to all the factors involved in the previous theories.

The HZFB model, shown in Figure 3.5.1, more approximates real system by treating it as a mixed connectivity composite.

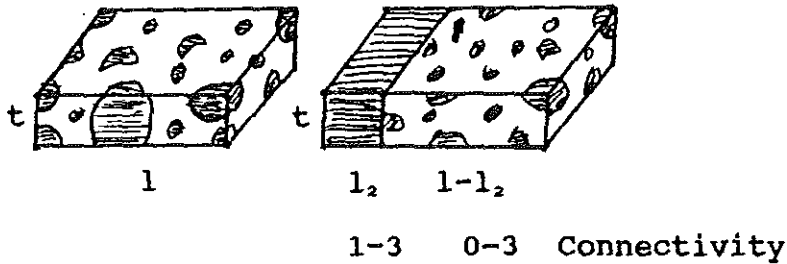


Fig. 3.5.1 The HFB equivalent model of a mixed connectivity composite. In the 1-3 connectivity region the PET particles are connected in one-dimensions. In the 0-3 connectivity region the PET particles are zero-dimensionally connected. The polymeric particles are connected in three-dimensions in both cases.

The elastic constant of the 1-3 connectivity region is c_2 . And the effective elastic constant of the 0-3 connectivity region is calculated using the BA type approximation²⁰(see section 2.5). To do this, first the corresponding elastic term of the depolarization field(in dielectricity) should be known.

Consider an inclusion of phase 2 in phase 1 shown in Figure 3.4.1 for the SPDT model. For isotropic and incompressible materials we have seen in sections 2.1 and 3.1 that the elastic and dielectric properties have one dimensional nature and have simple relations $T = cS$ and $D = \epsilon E$. Therefore, by use of the following substitution, previous discussions concerned with the dielectric property are valid for the elastic property^{2,4}.

$$\epsilon \rightarrow c, \quad E \rightarrow S \quad \text{and} \quad D \rightarrow T,$$

where ϵ is dielectric constant, c is elastic constant, E is electric field, D is dielectric displacement, S is strain and T is stress.

By analogy to the depolarization field, for fields in phases 1 and 2 we can write,

$$S_2 = S_1 + S^R \quad (3.5.1)$$

And S^R is given by²⁰,

$$S^R = -n(c_2 - c_1)S_1 / ((A(1-n)c_1 + nc_2)) \quad (3.5.2)$$

where A is a constant to be determined.

In the two phase dispersion system both strain S and stress T are additive.

$$S = fS_2 + (1-f)S_1 \quad (3.5.3)$$

and

$$T = fT_2 + (1-f)T_1 \quad (3.5.4)$$

where f is the PZT volume fraction.

Using the expressions for the elastic constants of the single phases,

$$T_1 = c_1S_1 \quad (3.5.5)$$

and

$$T_2 = c_2S_2 \quad (3.5.6)$$

and of the composite

$$T = cS, \quad (3.5.7)$$

we can write eq. 3.5.4 as,

$$cS = fc_2S_2 + (1-f)c_1S_1 \quad (3.5.8)$$

Substituting the value of S_2 from eq.3.5.1, of S from eq. 3.5.3 and noting that $S_1 = S$, we get

$$c = c_1(A(1-n)c_1 + nc_2 + Af(1-n)(c_2 - c_1)) / (A(1-n)c_1 + nc_2 - nf(c_2 - c_1)) \quad (3.5.9)$$

Substituting $1/3$ for n in eq. 3.5.9 (consistent with the spherical

particles in the SPDT model) and comparing it with eq. 3.4.1 yields $A = 3/4$ and hence we have²⁰,

$$S^R = -4n(c_2 - c_1)S_1 / ((3(1-n)c_1 + 4nc_2)) \quad (3.5.10)$$

for the elasticity term analogous to the depolarization field in dielectricity. We use this equation now in the BA type treatment of elasticity.

The HZFB model, shown in Figure 3.5.3, consists of a random unit of both components (1 and 2) embedded in an effective medium. The two components are treated symmetrically and there is a phase inversion. This is an advantage over the SPDT model where one component is always solute and the other always solvent.

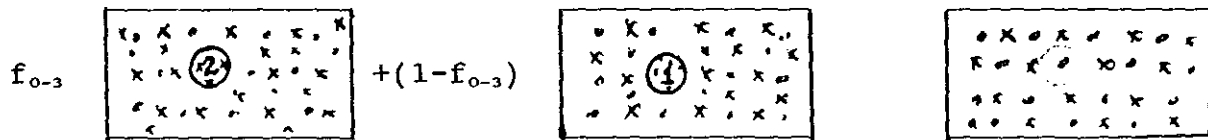


Fig. 3.5.2 The HZFB model of elasticity.

The strain inside the inclusions of the two components are given by

$$S_1 = S + S_1^R \text{ and } S_2 = S + S_2^R. \quad (3.5.11)$$

Using eq. 3.5.10, S_1^R and S_2^R are

$$S_2^R = -4n_2(c_2 - c_{0-3})S / (3(1-n_2)c_{0-3} + 4n_2c_2) \quad (3.5.12)$$

and

$$S_1^R = -4n_1(c_1 - c_{0-3})S / (3(1-n_1)c_{0-3} + 4n_1c_1) \quad (3.5.13)$$

Substituting the values of S_1 and S_2 from eq. 3.5.11 in 3.5.3, we get

$$S = f_{0-3}(S + S_2^R) + (1-f_{0-3})(S + S_1^R). \quad (3.5.14)$$

And substituting the values of S_1^R and S_2^R from eq. 3.5.12 and 3.5.13 in eq. 3.5.14, we get

$$[f_{0-3}(3 + n_2)c_{0-3}S/(3(1 - n_2)c_{0-3} + 4n_2c_2)] + \\ [(1 - f_{0-3})(3 + n_1)c_{0-3}S/(3(1 - n_1)c_{0-3} + 4n_1c_1)] = S \quad (3.5.15)$$

Cancelling S which appears both in the right hand side and left hand side of the equation, we get

$$[f_{0-3}(3 + n_2)c_{0-3}/(3(1 - n_2)c_{0-3} + 4n_2c_2)] + \\ [(1 - f_{0-3})(3 + n_1)c_{0-3}/(3(1 - n_1)c_{0-3} + 4n_1c_1)] = 1 \quad (3.5.16)$$

This is an expression for the effective elastic constant c of a two phase system in terms of the respective constants of the pure components (c_1 and c_2), the PZT volume fraction of the 0-3 connectivity region f_{0-3} and the geometric factors of the two phases (n_1 and n_2). The PZT volume fraction of the 1-3 connectivity region f_{1-3} is calculated using Monte Carlo method and the Pzt volume fraction of the 0-3 connectivity region f_{0-3} is calculated as $f - f_{1-3}$, where f is the total PZT volume fraction

3.6 PRESENT INVESTIGATION OF ELASTICITY

In our work we have considered the HZFB theory but ignored the concept of connectivity. In this work both phases are treated symmetrically and there is a phase inversion. This is an advantage over the SPDT theory of elasticity where one component is always solute and the other is always solvent and as a result making its predictions poor in the middle volume fraction range. Our work is a simplified HZFB theory where all the discussions concerned with the 0-3 connectivity composite are used for the whole system. And thus obtaining an expression similar to eq. 3.5.16.

4. PIEZOELECTRICITY

4.1 INTRODUCTION

In chapters 2 and 3 we have seen the dielectric and elastic properties of composite materials. In this chapter we will discuss the piezoelectric property of composite materials. The piezoelectric effect is an electro-mechanical effect in which the electric variables—electric field \mathbf{E} and dielectric displacement \mathbf{D} —are related to the mechanical variables—stress \mathbf{T} and strain \mathbf{S} .

We begin with some discussion of the relevant thermodynamics of piezoelectricity. The stress T_{ik} and strain S_{ik} tensors are related to the free energy F as²¹,

$$T_{ik} = (\partial F / \partial S_{ik})_{T,E} \quad (4.1.1)$$

where T (without suffix) is temperature and \mathbf{E} is electric field. Accordingly, the thermodynamic relation for the differential dF is

$$dF = -SdT + T_{ik}dS_{ik} - D_i dE_i \quad (4.1.2)$$

where S without suffix is entropy and \mathbf{D} is dielectric displacement.

The independent variables in eq. 4.1.2 include the components of the tensor S_{ik} . It is sometimes convenient to use instead of the components T_{ik} . To do so, we must introduce the thermodynamic potential, defined as

$$\phi = F - S_{ik}T_{ik} \quad (4.1.3)$$

For the differential of this quantity we have

$$d\phi = -SdT - S_{ik}dT_{ik} - D_i dE_i \quad (4.1.4)$$

The use of the thermodynamic potential ϕ here in accordance with eqs. 4.1.3 and 4.1.4 rests on the validity of eq. 4.1.1 and so is possible only for piezoelectric bodies.

Having defined the necessary thermodynamic quantities, let us now see the piezoelectric properties of crystals. If T_{ik} and E_k are taken as independent variables, the dielectric displacement D must be regarded as a function of them, and an expansion of this function must include the linear terms in them. The linear terms in the expansion of the components of a vector in powers of the components of a tensor of rank two can be written, in the most general case, as $\gamma_{ikl}T_{kl}$, where the constants γ_{ikl} form a tensor of rank three. The constant γ_{ikl} is called the piezoelectric tensor. If it is known, the piezoelectric properties of the material are entirely determined.

Adding the piezoelectric term in eq.2.1.3 for the dielectric displacement in the crystal, we have

$$D_i = D_{0i} + \epsilon_{ik}E_k + \gamma_{ikl}T_{kl}. \quad (4.1.5)$$

Corresponding additional terms appear in the thermodynamic quantities. The thermodynamic potential of a non-piezoelectric crystal in the absence of a field is, $\phi = \phi_0 - c_{ikln}T_{ik}T_{ln}$, where ϕ_0 pertains to undeformed body, and the second term is the ordinary elastic energy, determined by the elastic constant tensor c_{ikln} . For a piezoelectric we have

$$\phi = \phi_0 - c_{ikln}T_{ik}T_{ln} - \epsilon_{ik}E_iE_k - E_iD_{0i} - \gamma_{ikl}E_iT_{kl}. \quad (4.1.6)$$

The form of the last three terms is given by the fact that the derivatives of ϕ with respect to E_i (for a given temperature and

internal stress), found from the relation $D_i = -\partial\Phi/\partial E_i$, must accord with eq. 4.1.5.

Knowing Φ , we can obtain from eq. 4.1.4 a formula giving the strain tensor in terms of the stresses T_{ik} and the field E :

$$S_{ik} = -(\partial\Phi/\partial T_{ik})_{T,E} = C_{iklm}T_{lm} + \gamma_{ikl}E_l \quad (4.1.7)$$

It should be mentioned that to regard the quantities c_{iklm} and ϵ_{ik} for a piezoelectric as elastic constants and dielectric constants is somewhat conventional. With the definitions used here, they give respectively the strains as functions of elastic stresses for a given field, and the dielectric displacement as function of the field for given stresses. If, however, the deformation occurs with a given value of dielectric displacement, or we consider the dielectric displacement as a function of the field for given strains, the elastic constants and the dielectric constant will be represented by other quantities, which can be expressed as somewhat complex functions of the components of the tensors C_{iklm} , ϵ_{ik} and γ_{ikl} .

Now, let us consider which types of crystal symmetry which allow the existence of piezoelectricity; in other words, what are the restrictions imposed on the components of the tensor γ_{ikl} by symmetry conditions. In general, this tensor has 18 independent non-zero components, but in reality the number of independent components is usually much smaller.

In all symmetry transformations of a given crystal, the components of the piezoelectric tensor γ_{ikl} must remain unaltered in value. Hence it follows at once that no piezoelectric body

can have a centre of symmetry. For, on reflection in the centre (that is change of sign of all three co-ordinates), the components of a tensor of rank three change sign.

Of the 32 crystal classes, only 20 allow piezoelectricity. These are:- rhombic system: D_2, C_{2v} ; tetragonal system: $D_4, D_{2d}, S_4, C_4, C_{4v}$; rhombohedral system: D_3, C_3, C_{3v} ; hexagonal system: $D_6, C_{3h}, D_{3h}, C_6, C_{6v}$; Cubic system: T, T_d ; triclinic system: C_1 ; and monoclinic system: C_s, C_2 .

And of the 20 crystal classes which allow piezoelectricity, only 10 classes show pyroelectricity. They are:- rhombic system: C_{2v} ; tetragonal system: C_4, C_{4v} ; rhombohedral system: C_3, C_{3v} ; hexagonal system: C_6, C_{6v} ; triclinic system: C_1 ; and monoclinic system: C_s, C_2 . All pyroelectrics are piezoelectric. Pyroelectricity refers to the ability of a material to convert heat energy into electricity.

Coming back to the piezoelectric property, we will now define the four piezoelectric coupling coefficients (d, e, g and h). To start with the piezoelectric d constant, it is defined as

$$d_{ikl} = (\partial D_i / \partial T_{kl})_E \quad (4.1.8)$$

or

$$d_{ikl} = (\partial S_{ik} / \partial E_l)_T \quad (4.1.9)$$

where T_{kl} and S_{ik} are elements of stress and strain tensors acting on the composite, D_i and E_k are the dielectric displacement and the electric field, and d_{ikl} is piezoelectric coupling coefficient. High piezoelectric d constant is desirable for materials intended to develop motion or vibration, such as sonar or ultrasonic

cleaner transducers.

In chapters 2 and 3, we have assumed the composite materials to be isotropic and incompressible to obtain simple relations. As a result, both the dielectric and elastic properties have one dimensional nature. Applying these approximations here again will give one dimensional nature to the piezoelectric property too. Thus eq. 4.1.8 and 4.1.9 can be written as²⁻⁴

$$d = (\partial D / \partial T)_E = (\partial S / \partial E)_T. \quad (4.1.10)$$

Other piezoelectric coupling constants are defined in a similar way. For example, if the material is prevented from altering its shape by clamping, the application of a field will produce stress. This can be expressed as

$$e = (\partial D / \partial S)_E = (\partial T / \partial E)_S. \quad (4.1.11)$$

Another frequently used piezoelectric constant is the piezoelectric g constant,

$$g = (\partial E / \partial T)_D = (\partial S / \partial D)_T. \quad (4.1.12)$$

High piezoelectric g constant is required for materials intended to generate voltage in response to a mechanical stress, as in a phonograph pick-up.

If the stress is relieved by the material straining by an amount S , a fourth piezoelectric constant is

$$h = (\partial E / \partial S)_D = (\partial T / \partial D)_E \quad (4.1.13)$$

We may think of the boundary conditions: constant stress ($dT=0$), constant strain ($dS=0$), constant electric field ($dE=0$) and constant dielectric displacement ($dD=0$) as "free", "clamped", "short circuit", and "open circuit", respectively.

The units of the four piezoelectric constants follow from their definitions and therefore d is in m/V or in C/N , e is in N/V-m or in C/m^2 , g is in V-m/N or in m^2/C and h is in V/m or in N/C .

Section 4.2 is devoted to the local field coefficients which are important when we come to the calculation of the four piezoelectric constants which will be dealt with in section 4.3.

4.2 LOCAL FIELD COEFFICIENTS

In this section the local field coefficient is defined and the expressions for the local field coefficients for four models, namely, the series model, the parallel model, the spherical particles dispersion theory and the Habtamu Zewdie-F. Brouers type model are derived.

If an electric field E is applied to a two phase system, what will be the value of the field in the inclusions? We have answered this in section 2.4 (eq. 2.4.2) for an SPDT model. Eq. 2.4.2 is when an electric field E is applied to a two phase spherical dispersion system. We had,

$$E_2 = 3\epsilon_1 E / (2\epsilon_1 + \epsilon_2).$$

We see that $E_2 \neq E$. There is a coefficient for to equalize it to E_2 . This coefficient is defined as the local field coefficient with respect to the electric field. In general, for a field F we have

$$F_1 = L_{r1} F \tag{4.2.1}$$

where L_{r1} is the local field coefficient with respect to the field F . The field F can be electric field E , the dielectric

displacement D , the stress T or the strain S . Accordingly, we have

$$E_i = L_{Ei} E_i, \quad (4.2.2)$$

$$S_i = L_{Si} S_i, \quad (4.2.3)$$

$$D_i = L_{Di} D_i, \quad (4.2.4)$$

$$\text{and } T_i = L_{Ti} T_i. \quad (4.2.5)$$

Since $D = \epsilon E$ and $T = cS$, we will have

$$\epsilon_i E_i = L_{Di} \epsilon E$$

$$\text{or } L_{Di} = \epsilon_i L_{Ei} / \epsilon, \quad (4.2.6)$$

$$\text{and } c_i S_i = L_{Ti} c S$$

$$\text{or } L_{Ti} = c_i L_{Si} / c \quad (4.2.7)$$

Substituting the values of E_i and E , and S_i and S for the four theories, namely, the series model, the parallel model, the SPDT and the HZFB type model in eqs. 4.2.2 and 4.2.3 we get the expressions given in below for L_{Ei} and L_{Si} . The expressions for the L_{Di} and L_{Ti} are derived using eqs. 4.2.6 and 4.2.7, respectively.

Series model local field coefficients:

$$L_{Ei} = \epsilon / \epsilon_i \quad L_{Di} = 1 \quad (4.2.8)$$

$$L_{Si} = c / c_i \quad L_{Ti} = 1 \quad (4.2.9)$$

Parallel model local field coefficients

$$L_{Ei} = 1 \quad L_{Di} = \epsilon_i / \epsilon \quad (4.2.10)$$

$$L_{Si} = 1 \quad L_{Ti} = c_i / c \quad (4.2.11)$$

SPDT model local field coefficients:

$$L_{E2} = 3\epsilon_1 / (2\epsilon_1 + \epsilon_2 + f(\epsilon_1 - \epsilon_2)) \quad (4.2.12)$$

$$L_{E1} = (2\epsilon_1 + \epsilon_2) / (2\epsilon_1 + \epsilon_2 + f(\epsilon_1 - \epsilon_2)) \quad (4.2.13)$$

$$L_{D2} = 3\epsilon_2 / (2\epsilon_1 + \epsilon_2 - 2f(\epsilon_1 - \epsilon_2)) \quad (4.2.14)$$

$$L_{D1} = (2\epsilon_1 + \epsilon_2) / (2\epsilon_1 + \epsilon_2 - 2f(\epsilon_1 - \epsilon_2)) \quad (4.2.15)$$

$$L_{S2} = 5c_1 / (3c_1 + 2c_2 + 2f(c_1 - c_2)) \quad (4.2.16)$$

$$L_{S1} = (3c_1 + 2c_2) / (3c_1 + 2c_2 + 2f(c_1 - c_2)) \quad (4.2.17)$$

$$L_{T2} = 5c_2 / (3c_1 + 2c_2 - 3f(c_1 - c_2)) \quad (4.2.18)$$

$$L_{T1} = (3c_1 + 2c_2) / (3c_1 + 2c_2 - 3f(c_1 - c_2)) \quad (4.2.19)$$

HZFB type model local field coefficients:

$$L_{E1} = \epsilon / ((1-n_1)\epsilon + n_1\epsilon_1) \quad (4.2.20)$$

$$L_{D1} = \epsilon_1 / ((1-n_1)\epsilon + n_1\epsilon_1) \quad (4.2.21)$$

$$L_{S1} = (3+n_1)c / (3(1-n_1)c + 4n_1c_1) \quad (4.2.22)$$

$$L_{T1} = (3+n_1)c_1 / (3(1-n_1)c + 4n_1c_1) \quad (4.2.23)$$

These expressions for the various local field coefficients will be used to evaluate the piezoelectric coupling constants d , e , g and h for the four models in the next section (i.e. section 4.3).

4.3 PIEZOELECTRIC CONSTANTS

In this section expressions for the four piezoelectric coupling constants d , e , g and h of composite materials will be derived from the local field coefficients and the piezoelectric constants of the pure components.

When the inclusions in a composite are piezoelectric, we can observe piezoelectric effects as a gross property of the composite. In order to relate the gross piezoelectric constants to the piezoelectric constant of the inclusions, it is assumed that, the piezoelectric constants of the inclusions are one-

dimensional and relate the dielectric variables along one polar axis and the elastic variables along the directions perpendicular(or parallel) to the polar axis.

The direct piezoelectric effect(for example applying strain S to get dielectric displacement D) for a composite may be divided into three processes:

- (a). The strain S applied to a composite produces local strain S_i in piezoelectric inclusion(phase i).
- (b). S_i gives rise to the dielectric displacement D_i in phase i due to the piezoelectric effect of the inclusions with the piezoelectric constant e_i .
- (c). D_i is observed as an increase of macroscopic dielectric displacement D .

Thus for the piezoelectric e constant, we have²

$$e = D/S.$$

$$\begin{aligned} \text{And } e &= (S_i/S)(D_i/S_i)(D/D_i) \\ &= L_{Si} e_i (1/L_{Di}) \end{aligned} \quad (4.3.1)$$

where L_{Si} and L_{Di} are the local field coefficients with respect to the strain and the dielectric displacement, respectively and e_i is the piezoelectric constant of pure phase i .

The piezoelectric converse effect may also be divided into three processes:

- (a). The applied electric field E to a composite produces local electric field E_i in phase i .
- (b). E_i gives rise to the local stress T_i in phase i due to the piezoelectric effect of the inclusions with piezoelectric

constant i .

(c). T_i is observed as an increment of macroscopic stress T .

Thus for the piezoelectric e constant, we have^{2,4}

$$\begin{aligned} e &= (T/E) \\ e &= (T/T_i) (T_i/E_i) (E_i/E) \\ &= (1/L_{TA}) (e_i) (L_{EA}) \end{aligned} \quad (4.3.2)$$

Similarly, the other piezoelectric constants are,

$$d = (L_{Ti}/L_{Di}) d_i = (L_{Ei}/L_{Si}) d_i \quad (4.3.3)$$

$$g = (L_{Ti}/L_{Ei}) g_i = (L_{Di}/L_{Si}) g_i \quad (4.3.4)$$

$$h = (L_{Si}/L_{Ei}) h_i = (L_{Di}/L_{Ti}) h_i. \quad (4.3.5)$$

In general, for a composite made up of any number of phases, we have

$$d = \bar{\Sigma} (L_{Ti}/L_{Di}) d_i = \bar{\Sigma} (L_{Ei}/L_{Si}) d_i \quad (4.3.6)$$

$$e = \Sigma (L_{Si}/L_{Di}) d_i = \Sigma (L_{Ei}/L_{Ti}) d_i \quad (4.3.7)$$

$$g = \Sigma (L_{Ti}/L_{Ei}) g_i = \Sigma (L_{Di}/L_{Si}) g_i \quad (4.3.8)$$

$$h = \Sigma (L_{Si}/L_{Ei}) h_i = \Sigma (L_{Di}/L_{Ti}) h_i. \quad (4.3.9)$$

Previous expressions^{2,5,20} for the four piezoelectric coupling constants were

$$d = fL_{T2}L_{E2}d_2 \quad (4.3.10)$$

$$e = fL_{S2}L_{E2}d_2 \quad (4.3.11)$$

$$g = fL_{T2}L_{D2}g_2 \quad (4.3.12)$$

$$h = fL_{S2}L_{D2}h_2 \quad (4.3.13)$$

These four equations (eqs. 4.3.10-4.3.13) were derived on the assumption that the dielectric displacement at zero electric field is zero, which is not true for ferroelectric ceramic-polymer composite materials.

The four equations (eqs. 4.3.6-4.3.9) are used to interpret experimental data on piezoelectric properties of composite materials (see section 5). They are used both for the spherical particle dispersion theory (SPDT) model (using eqs. 4.2.12-4.2.29 for the local field coefficients of the SPDT model) and the HZFB type models (using eqs. 4.2.20-4.2.23 for the local field coefficients of the HZFB type model).




To test the existing theories and the improved theories, we have compared the theoretical predictions with experimental data on a variety of composite materials in the next section (i.e. section 5).

5. RESULTS AND DISCUSSION

5.1 PROOFS OF THE THEORETICAL PREDICTIONS

The limits of the theoretical predictions of the effective dielectric and elastic constants (eqs. 2.5.7 and 3.6.1, respectively) and of the local field coefficients (eqs. 4.2.20-4.2.23) are investigated as a function of the geometric factors. The limits are when the geometric factor n takes its maximum value unity (for oblate shaped inclusions) and its minimum value zero (for prolate shaped inclusions). We expect the expressions (eq. 2.5.7, 3.6.1 and 4.2.20-4.2.23) to reduce to the parallel model expressions (eqs. 2.3.4, 3.3.4 and 4.2.10-4.2.11, respectively) when n is zero, to reduce to the series model expressions (eqs. 2.2.7, 3.2.7 and 4.2.8-4.2.9, respectively) when n is unity and to have intermediate values of properties for intermediate values of the geometric factors. This is expected because the parallel model is actually a combination of prolate shaped inclusions and the series model is a combination of oblate shaped inclusions. The geometric factor n for the different shapes of inclusions are:

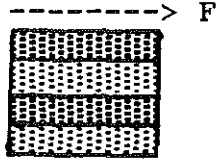
----->F

$n = 0$	prolate	
$n = 1/3$	sphere	
$n = 1$	oblate	

$0 < n < 1$ intermediate shapes

Combination of prolate shaped inclusions ($n=0$) gives the

parallel model,

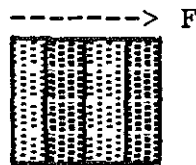


which is actually equivalent to a 1-1 connectivity model,



where F is the applied field.

And combination of oblate shaped inclusions ($n=1$) gives the series model



which is actually equivalent to a 2-2 connectivity model,



where F is the applied field.

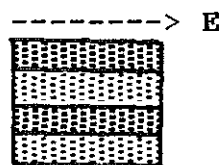
As expected the theoretical predictions (eqs. 2.5.7, 3.6.1 and 4.2.20-4.2.23) reduce to the parallel model expressions (eqs. 2.3.4, 3.3.4 and 4.2.10-4.2.11) when n is zero, to the series model expressions (eqs. 2.2.7, 3.2.7 and 4.2.8-4.2.9) when n is unity and take intermediate values for intermediate values of n . This is proof of the theoretical predictions. Therefore, the theoretical predictions (eqs. 2.5.7, 3.6.1 and 4.2.20-4.2.23)

could take care of the parallel and 1-1 connectivity models when n is zero, and the series and 2-2 connectivity models when n is unity. Thus the shape parameter n is an effective parameter which could take care of both the effect of shape of inclusions and the concept of connectivity.

5.2 THEORETICAL PREDICTIONS ON THE EFFECTS OF THE SHAPE OF INCLUSIONS.

As the shape of inclusions of a composite change the properties of the composite change. We can easily see this if we consider the following three cases: (i) Combination of prolate-shaped inclusions (the parallel model), (ii) Combination of oblate-shaped inclusions (the series model), and (iii) Combination of intermediate shaped inclusions (the other models such as SPDT, BA, and HZFB).

In the parallel model which corresponds to $n = 0$ in the theoretical predictions (eqs. 2.5.7, 3.6.1 and 4.2.20-4.2.23) we observe continuity of field. There is no screening of the field. For an applied electric field E , we have

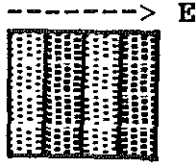


$$E = E_1 = E_2,$$

where 1 stands for phase 1 and 2 for phase 2. As a result the properties of the composite are expected to have maximum values.

In the series model which corresponds to $n = 1$ in the theoretical predictions (eqs. 2.5.7, 3.6.1 and 4.2.20-4.2.23),

there is maximum screening of the field.



And as a result, the properties of the composite are expected to have minimum values.

For intermediate-shaped inclusions (where $0 < n < 1$) the properties of composite materials are expected to have intermediate values.

Now we shall discuss specific models. Figures 5.1, 5.2, and 5.3 and show the dependence of the dielectric (ϵ), elastic (c) and piezoelectric (d) constants, respectively, on the volume fraction and geometric factors of the PZT and polymer phases. The values of the constants of the pure components, $\epsilon_1 = 8.9$, $\epsilon_2 = 1850$, $c_1 = 0.79 \text{ GN/m}^2$, $c_2 = 6.32 \text{ GN/m}^2$, $d_1 = 0 \text{ pC/N}$, and $d_2 = 180 \text{ pC/N}$ are used in the theoretical calculations where subscript 1 stands for the polymer phase and 2 stands for the PZT phase. The composite will have intermediate values but the PZT phase dominates in the parallel model and the polymer phase dominates in the series and the SPDT models. The figures 5.1, 5.2, and 5.3 are plots of the theoretical predictions of the dielectric constant (eq. 2.5.7), the elastic constant (eq. 3.6.1) and the piezoelectric d constant (eq. 4.2.20-4.2.23 in 4.3.6) of a lead zirconate titanate (PZT)-polyvinylidene fluoride (PVDF) composite against the

PZT volume fraction at different values of the geometric factors of the two phases n_1 and n_2 . In all the three figures, curve a is when $n_1 = n_2 = 0.01$, which is equivalent to the parallel model and the 1-1 connectivity model, and has maximum values of properties, as expected. Curve e is when $n_1 = n_2 = 0.99$, which is equivalent to the series model and the 2-2 connectivity model, and has minimum values of properties, as expected here again. Curves c, d and e are when n_1 and n_2 take intermediate values and has intermediate values of properties. This is in agreement with what we have expected from the discussions of in previous paragraphs.

This clearly demonstrate that the shape of inclusions greatly affect the dielectric, elastic, and piezoelectric properties of composite materials. It shows the importance of considering the effect of shape of inclusions in the study of the properties of composite materials.

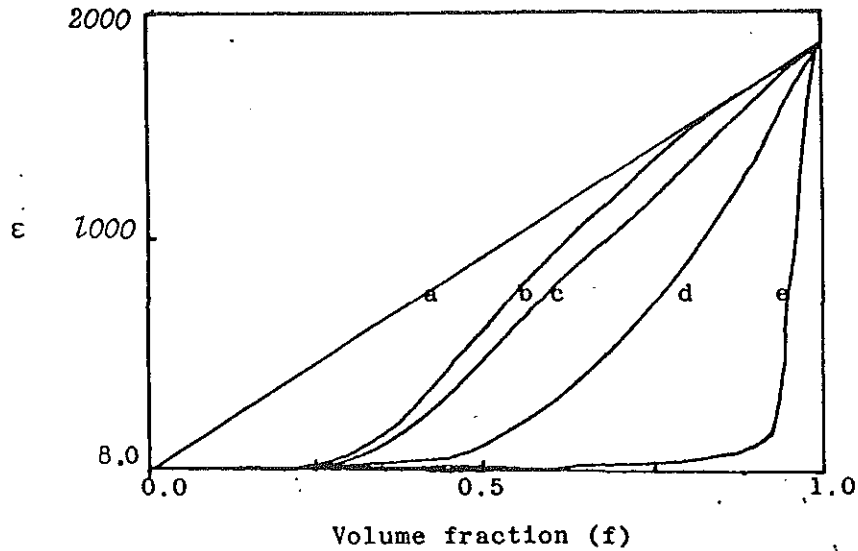


Fig. 5.1: Effect of shape of inclusions on the dielectric constant(ϵ) of a PZT-PVDF composite.(eq. 2.5.7)

	$\frac{n_1}{n_2}$	$\frac{n_2}{n_1}$
a) Parallel model	.01	.01
b) Spherical matrix	.33	.51
c) Spherical model	.33	.33
d) Spherical inclusions	.51	.33
e) Series model	.99	.99

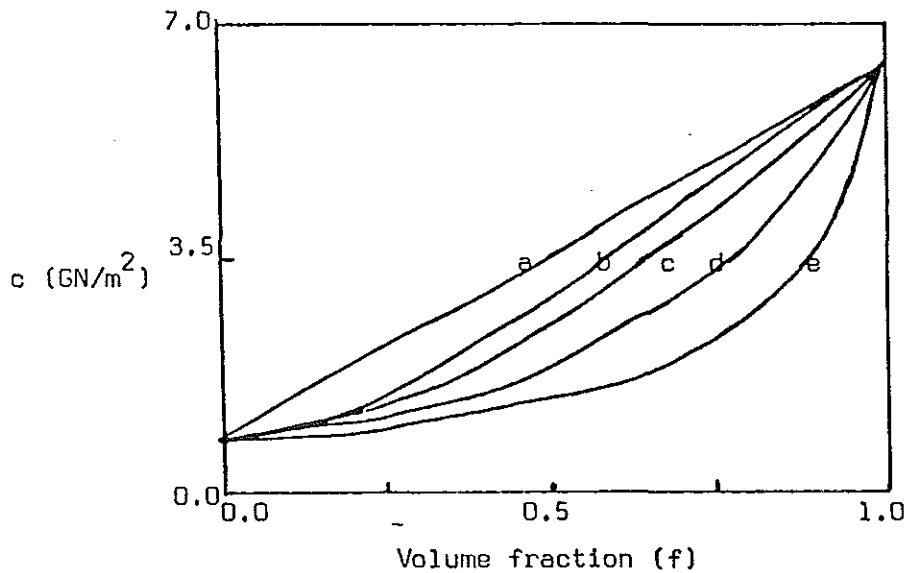


Fig. 5.2: Effect of shape of inclusions on the elastic constant(c) of a PZT-PVDF composite. (eq. 3.6.1)

	$\frac{n_1}{n_2}$	$\frac{n_2}{n_1}$
a) Parallel model	.01	.01
b) Spherical matrix	.33	.51
c) Spherical model	.33	.33
d) Spherical inclusions	.51	.33
e) Series model	.99	.99

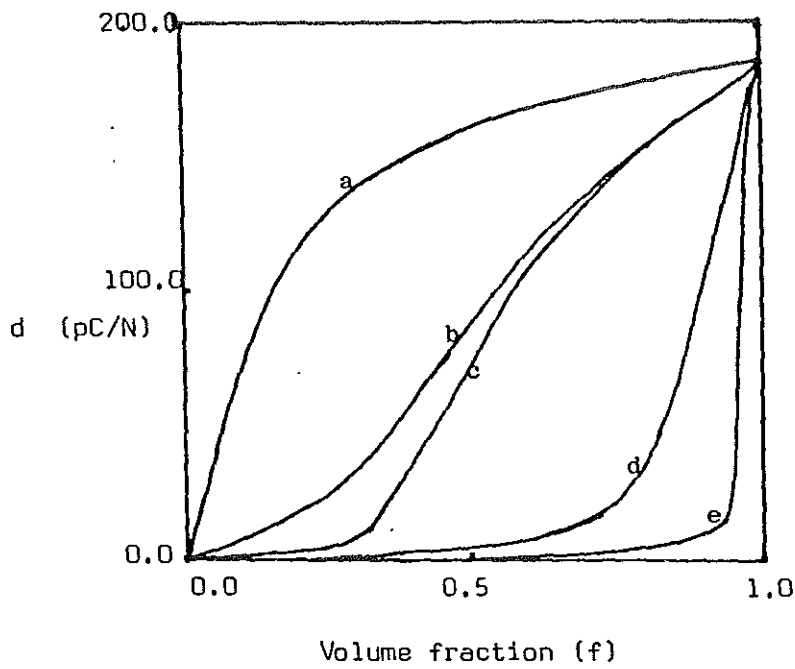


Fig. 5.3: Effect of shape of inclusions on the piezoelectric d constant of a PZT-PVDF composite (eq. 4.3.6)

	$\frac{n_1}{n_2}$	$\frac{n_2}{n_1}$
a) Parallel model	.01	.01
b) Spherical matrix	.33	.05
c) Spherical model	.33	.33
d) Spherical inclusions	.81	.33
e) Series model	.99	.99

We have also studied the properties of composite materials against the geometric factors of the two components at fixed volume fraction of PZT. The purpose of this study were: (i) to see if the effects of the geometric factors of the two components are of equal magnitude, or not, (ii) to see if the effects of the geometric factors of the two components for the dielectric constant($n_{1\epsilon}$ and $n_{2\epsilon}$) and those of the elastic constant(n_{1e} and n_{2e}) are of equal magnitude or not, and (iii) to suggest optimum conditions for the composite which gives it flexibility and high piezoelectric activity.

From figures 5.4-5.9 , which are plots of the theoretical predictions(eq. 2.5.7 for the dielectric constant, 3.6.1 for the elastic constant, and 4.2.20-4.2.23 in 4.3.6 for the piezoelectric d constant) versus the geometric factors of the two components n_1 and n_2 at fixed PZT volume fraction f), we conclude that:

(i) The geometric factor of the component with volume fraction is more effective. This means that for low PZT volume fraction the effect of n_2 is predominant and for high PZT volume fraction n_1 is predominant. 2 stands for the PZT phase(phase 2) and 1 stands for the polymer phase(phase 1).

(ii) The piezoelectric d constant of composite materials strongly depend on the geometric factors of the two components for the dielectric constant($n_{1\epsilon}$ and $n_{2\epsilon}$) and depends less on the those of the elastic constant(n_{1e} and n_{2e}), and

(iii) The PZT-polymer composite with $n_2 \approx 0.15$, $n_1 \approx 0.33$ and high PZT volume fraction f will be flexible and have high piezoelectric activity. This is because for n_1 and n_2 near to zero (the parallel model) the composite will have high piezoelectric activity but will not be flexible. For n_1 and n_2 near to unity (the series model) the composite will not be flexible and will have low piezoelectric activity. For n_1 near to zero and n_2 near to unity (pure PZT) the composite will have high piezoelectric activity but will be brittle. And for n_1 near to unity and n_2 near to zero (pure polymer) the composite will be flexible but will have low piezoelectric activity. But it will have high piezoelectric activity and flexibility for n_2 around 0.15 and n_1 around 0.33 and high f .

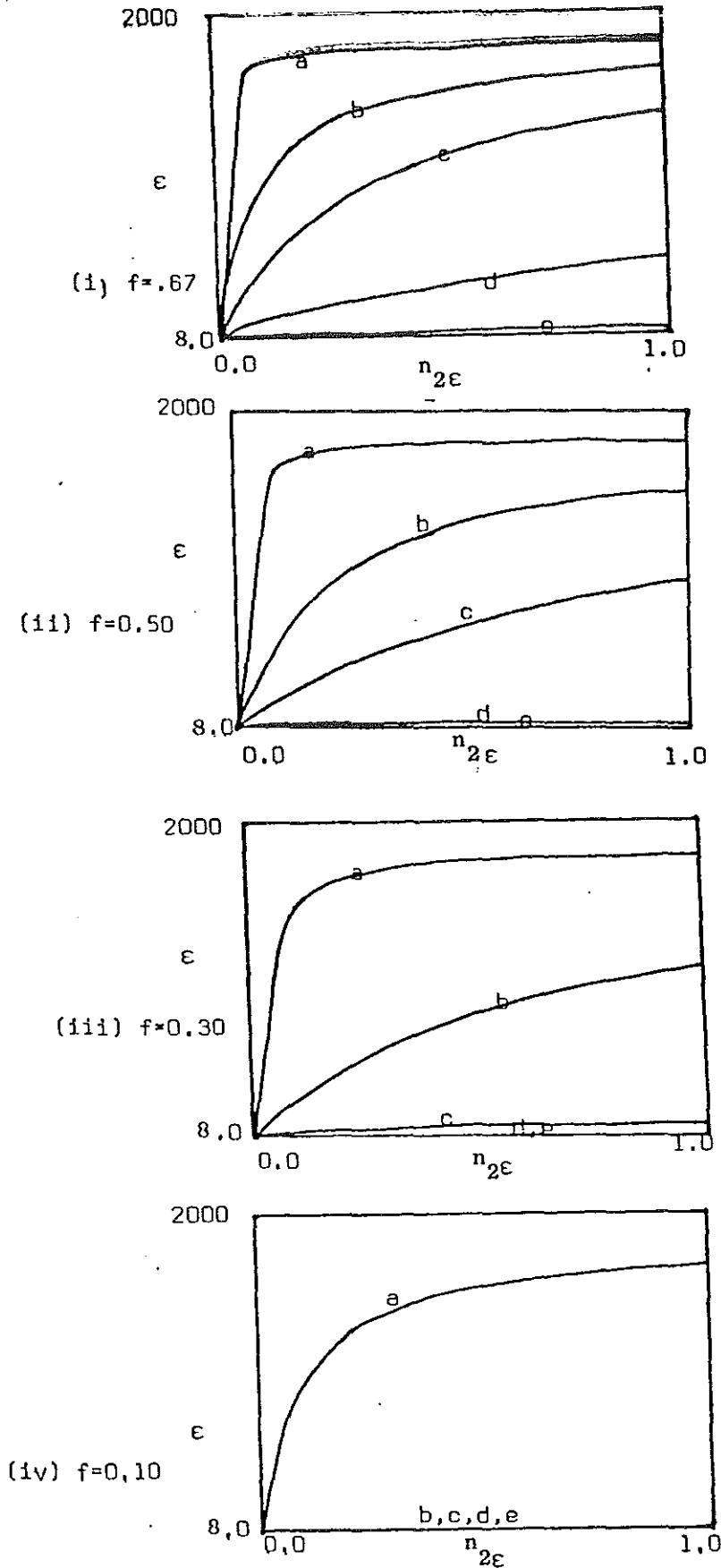


Fig. 5.4 : PZT volume fraction(f) and geometric factor(n) dependence of the dielectric constant(ϵ)of a PZT-PVDF composite. In the figures: $n_{2\epsilon}$ =geometric factor for the PZT phase and $n_{1\epsilon}$ =geometric factor for the PVDF phase. $n_{1\epsilon}$ has values .01, .15, .33, .61 and .91 for curves a,b,c,d and e respectively.

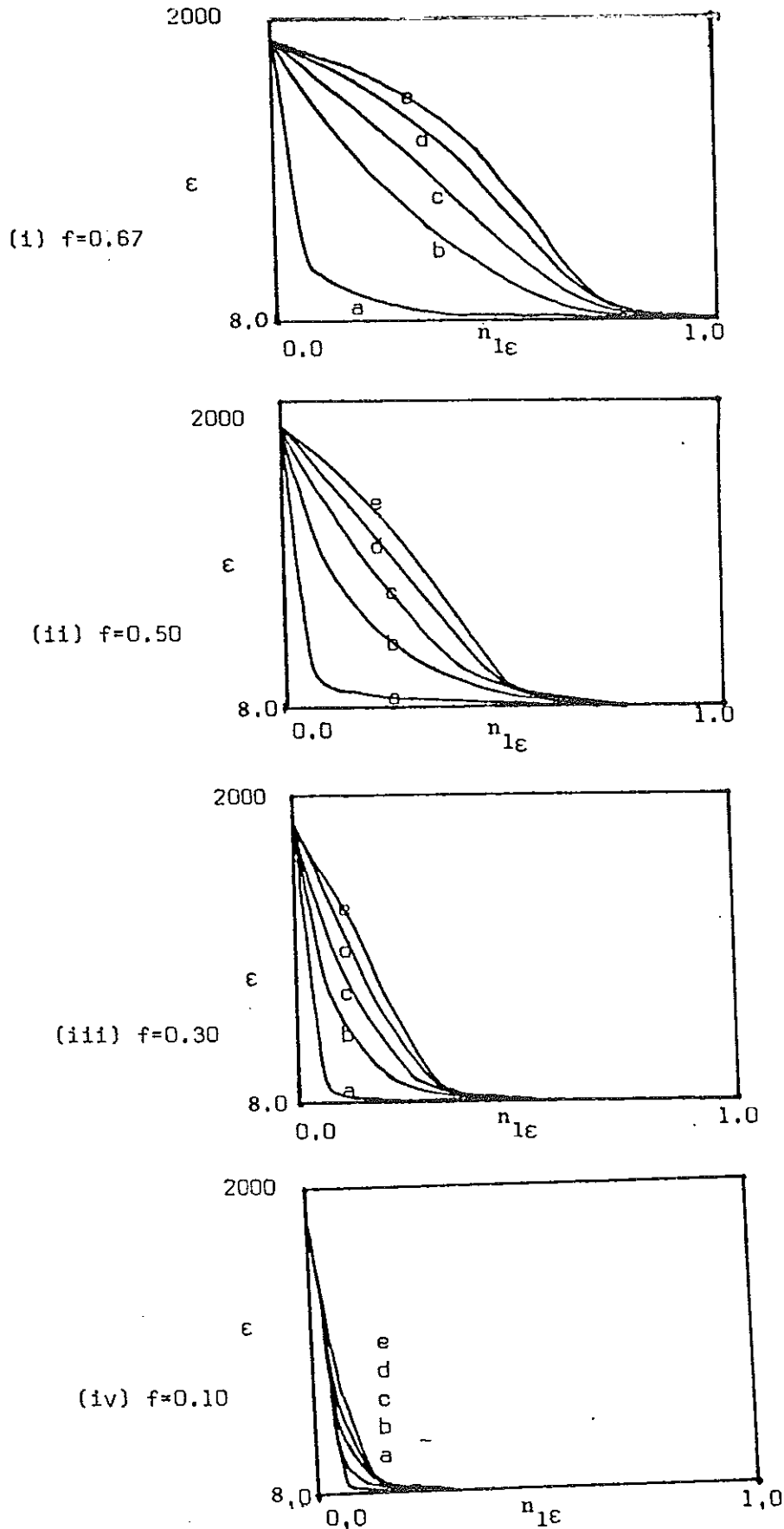


Fig. 5.5 : PZT volume fraction(f) and geometric factor(n) dependence of the dielectric constant(ϵ) of a PZT-PVDF composite. In the figures: $n_{1\epsilon}$ =geometric factor for the PVDF phase and $n_{2\epsilon}$ = geometric factor for the PZT phase, $n_{2\epsilon}$ has value ,01, ,15, ,33, ,61 and ,91 for curves a,b,c,d and e respectively.

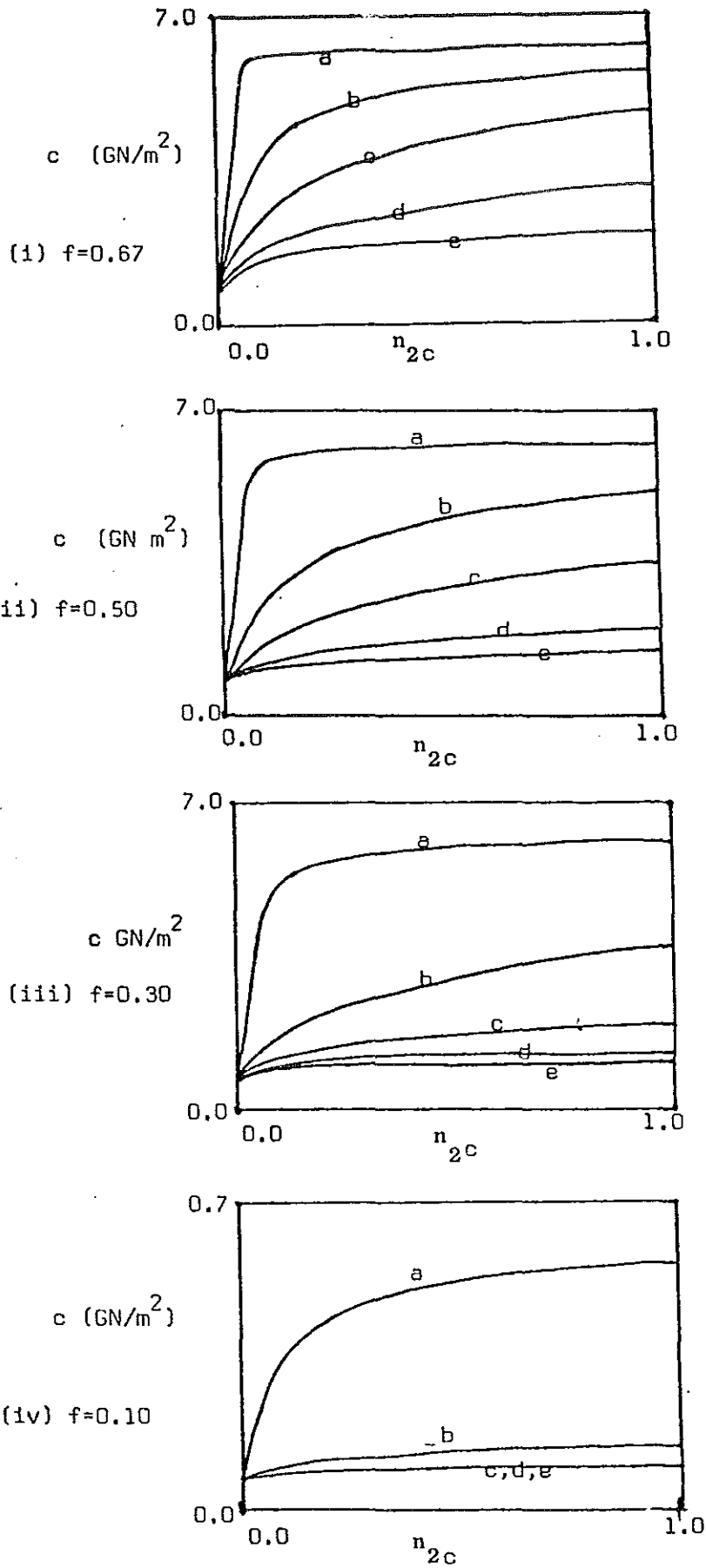


Fig. 5.6 : PZT volume fraction(f) and geometric factor(n) dependence of the elastic constant(c) of a PZT-PVDF composite. In the figures: n_{2c} = geometric factor for the PZT phase and n_{1c} = geometric factor for the PVDF phase. n_{1c} has values 0.01, 0.15, 0.33, 0.61 and 0.99 for curves a, b, c, d and e resp.

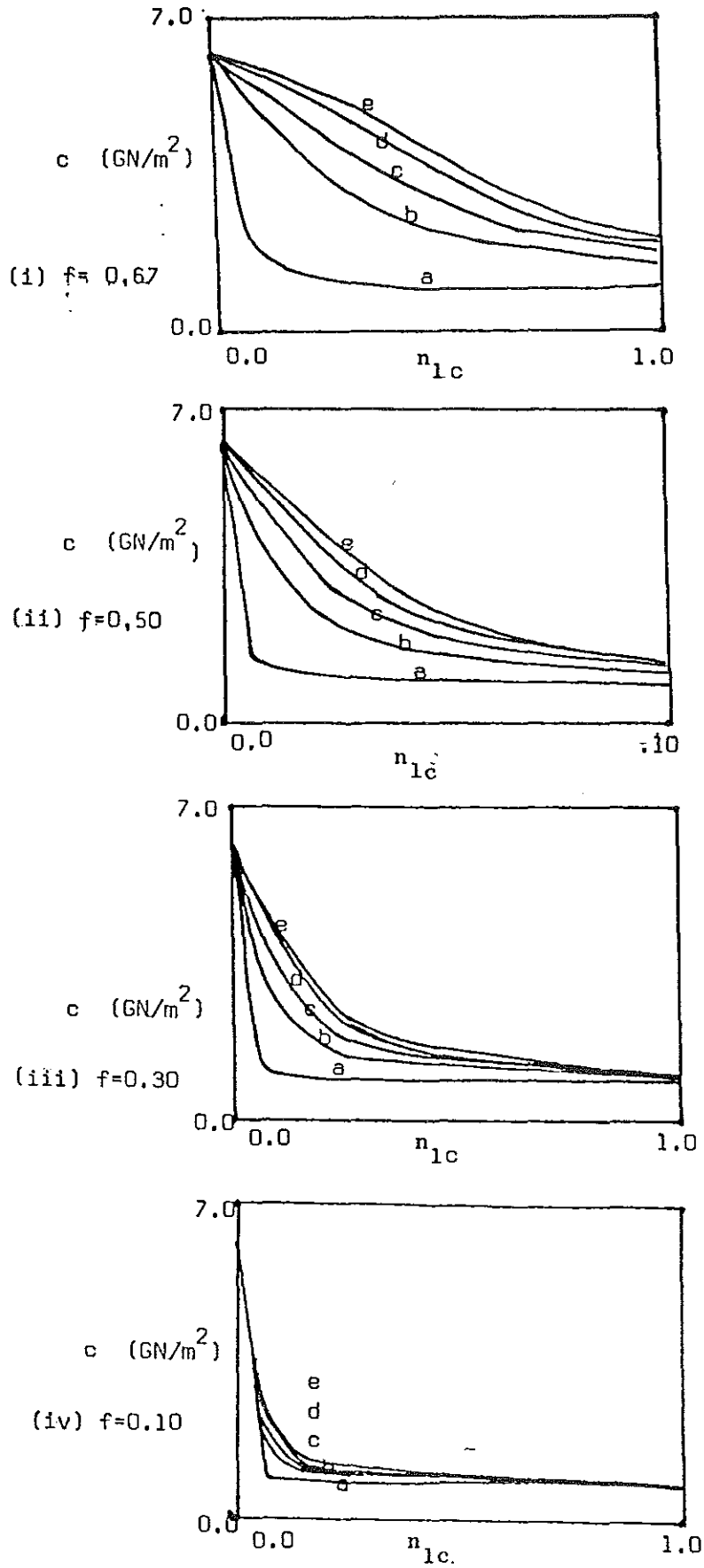


Fig. 5.7 : PZT volume fraction(f) and geometric factor(n) dependence of the elastic constant(c) of a PZT-PVDF composite. In the figures, n_{2c} and n_{1c} are the geometric factors for the PZT and the PVDF phases, respectively. n_{2c} has values 0.01, 0.05, 0.1, 0.15, 0.2 for curves a, b, c, d and e respectively.

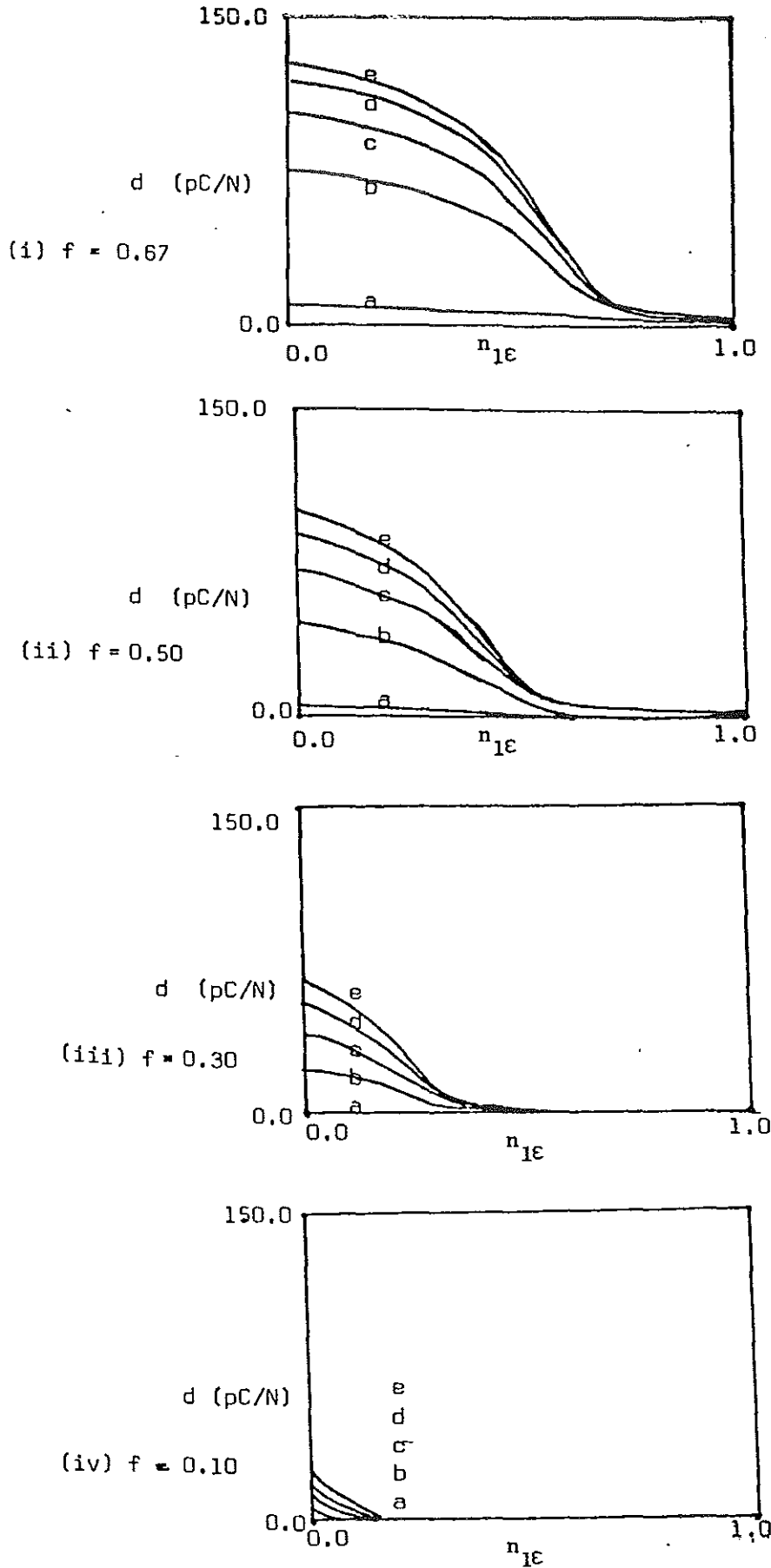


Fig. 5.8 : PZT volume fraction(f) and geometric factor(n) dependence of the piezoelectric d constant of a PZT-PVDF composite. In the figures, n_{2c} , n_{1c} , n_{2c} and n_{1c} stand for the geometric factors of the PZT and the PVDF phases, (2 = PZT, 1 = PVDF). n_{1c} has values 0.01, .15, .33, .61 and .91 for curves a,b,c,d and e respectively. $n_{2c} = 0.50$ and $n_{2c} = 0.50$ for all the curves, while n_{1c} is varied from 0.0 to 1.0.

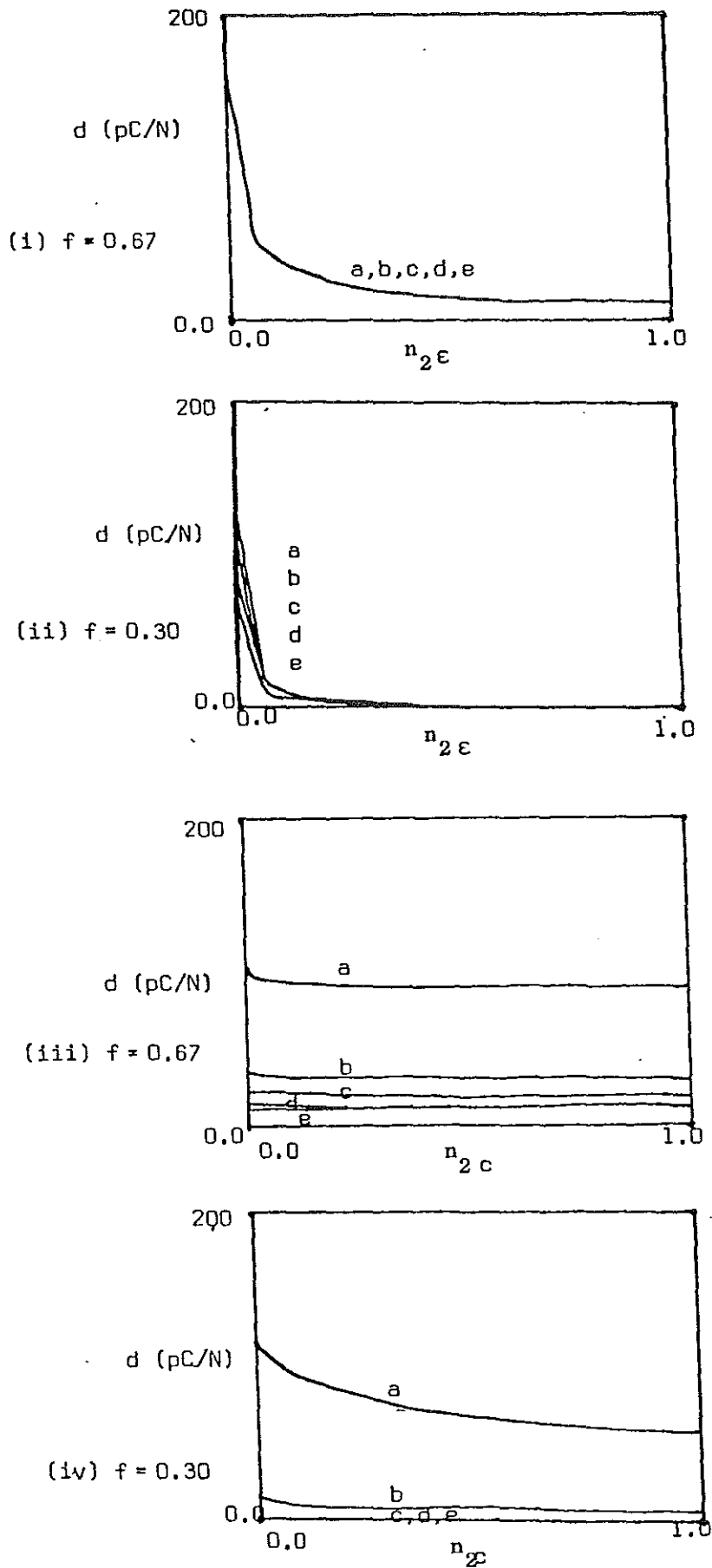


Fig. 5.9 : PZT volume fraction(f) and geometric factor(n) dependence of the piezoelectric d constant of a PZT-PVDF composite. In figures (i) and (ii): $n_{1\epsilon} = 0.70$, $n_{1c} = 0.50$ and $n_{2\epsilon}$ has values .01, .15, .33, .61 and .91 for curves a,b,c,d and e respectively; while n_{2c} is varied from 0.0 to 1.0. In figures (iii) and (iv): $n_{1\epsilon} = 0.70$, $n_{1c} = 0.50$ and $n_{2\epsilon}$ has values .01, .15, .33, .61 and .91 for curves a,b,c,d, and e

5.3 COMPARISON WITH EXPERIMENTAL DATA.

(VOLUME FRACTION DEPENDENCE)

In sections 5.1 and 5.2 we have seen that the theoretical predictions (eqs. 2.5.7 for the dielectric constant, 3.6.1 for the elastic constant and 4.2.20-4.2.23 in 4.3.6-4.3.9 for the piezoelectric constants) could take care of the series and the parallel models (when $n = 1$ and $n = 0$, respectively) and the connectivity models, 2-2 and 1-1, respectively. That is by varying the values of the geometric factors n_1 and n_2 between zero and unity, we can make the predictions fit experimental data on different types of connectivity models.

In this section, the theoretical predictions (eqs. 2.5.7 for the dielectric constant, 3.6.1 for the elastic constant and 4.2.20-4.2.23 in 4.3.6 for the piezoelectric d constants) and the predictions of the spherical particles dispersion theory (SPDT) (eqs. 2.4.9 for the dielectric constant, 3.4.1 for the elastic constant and 4.2.12-4.2.19 in 4.3.6 for the piezoelectric d constant) are tested on experimental data of a variety of composite materials.

In section 5.3.1 we test the theoretical predictions on a 0-3 connectivity composite whose piezoelectric activity comes only from the PZT phase (phase 2). In section 5.3.2 we will test the theoretical predictions on a 0-3 connectivity composite whose both phases are piezoelectrically active. And in section 5.3.3 the theoretical predictions are tested on a 1-1 and 1-3

connectivity composite whose piezoelectric activity comes only from the PZT phase(phase 2). In all the three sections we have plots of the property(dielectric, elastic, and piezoelectric) versus the PZT volume fraction.

5.3.1 TEST ON 0 - 3 CONNECTIVITY COMPOSITE WHERE ONLY THE PZT PHASE IS PIEZOELECTRICALLY ACTIVE

In this section, the theoretical predictions(eqs. 2.5.7 for the dielectric constant, 3.6.1 for the elastic constant and 4.2.20-4.2.23 in 4.3.6 for the piezoelectric d constant) and the predictions of the spherical particles dispersion theory(SPDT)(eqs. 2.4.9 for the dielectric constant, 3.4.1 for the elastic constant and 4.2.12-4.2.19 in 4.3.6 for the piezoelectric d constant) are tested on experimental data of the dielectric, elastic and piezoelectric constants at different volume fractions taken from Furukawa *et al*².

The composite system is a lead zirconate titanate(PZT)-polyvinylidene fluoride(PVDF) system. The PZT powder is expected to have on the average spherical shape and to be homogeneously distributed in the polymer matrix.

5.3.1.1 THE DIELECTRIC CONSTANT

Here, the theoretical prediction(eq. 2.5.7) and the SPDT prediction(eq. 2.4.9) for the dielectric constant are tested on experimental data of a 0-3 connectivity composite. This is shown in Figure 5.10, which is a plot of the dielectric constant ϵ

versus the PZT volume fraction. In the figure, points are experimental data, the dashed line is the SPDT prediction (eq. 2.4.9) and the solid line is the theoretical prediction (eq. 2.5.7). The dielectric constants of the pure PZT and polymer 1850 and 8.9, respectively, are used in the theoretical calculations. The composite is expected to have intermediate values and to be dominated by the polymer phase.

We have seen in section 2.4 that the SPDT prediction does not involve shape parameter. In other words, the effect of shape of inclusions are ignored in the SPDT predictions. In addition, the model treats one component always as a solute and the other always as a solvent. As a result, the predictions of the SPDT are expected to be poor in the middle volume fraction range where there can be percolation. This is exactly what we see in Fig. 5.10 (the dashed line).

The theoretical prediction in section 2.5 (eq. 2.5.7) include the effect of shape of inclusions and at the same time the model treats both components symmetrically and as a result the role of inclusion and host interchanges as the composition changes. As a result, the prediction by eq. 2.5.7 is expected to agree better with experimental data than do the SPDT prediction (eq. 2.4.9). This is seen in Fig. 5.10 (the solid line). The values of the geometric factors 0.03 for $n_{2\epsilon}$ and 0.35 for $n_{1\epsilon}$ are found to best fit the theoretical prediction of the dielectric constant eq. 2.5.7 with experimental data taken from Furukawa *et al*² as shown in Fig. 5.10 (the solid line) with a correlation coefficient

of 0.99 which is significant at 0.001 α value. For a material prepared under different conditions the value of the geometric factors will be different. For uniformly distributed spherical inclusions n_{2c} and n_{1c} were expected to take values around 0.33. But n_{2c} is 0.03 which implies that the PZT particles are connected across the electrode. The specification in the sample preparation describes that the composite film was prepared by pressing perpendicular to the film surface. The PZT sample which has been once distributed homogeneously would make electrical contact in the normal direction to the surface of the film during the pressing process. Thus, the value of n_{2c} is consistent with this observation.

5.3.1.2 THE ELASTIC CONSTANT

In this section, the theoretical prediction (eq. 3.6.1) and the SPDT prediction (eq. 3.4.1) for the elastic constant are tested on experimental data of a 0-3 connectivity composite. This is shown in Figure 5.11, which is a plot of the elastic constant c versus the PZT volume fraction. In the figure, points are experimental data, the dashed line is the SPDT prediction (eq. 3.4.1) and the solid line is the theoretical prediction (eq. 3.6.1.). The elastic constants of the pure PZT and polymer 6.32 and 0.79 GN/m², respectively, are used in the theoretical calculations. The elastic constant of the composite is expected to have intermediate values and to be dominated by the polymer phase.

We have seen in section 3.4 that the SPDT prediction does not involve shape parameter. In other words, the effect of shape of inclusions are ignored in the SPDT predictions. In addition, the model treats one component always as a solute and the other always as a solvent. As a result, the predictions of the SPDT are expected to be poor in the middle volume fraction range where there can be percolation. This is exactly what we see in Fig. 5.11(the dashed line).

The theoretical prediction in section 3.6(eq.3.6.1) include the effect of shape of inclusions and at the same time the model treats both components symmetrically(there is a phase inversion at percolation threshold). As a result, the prediction by eq. 3.6.1 is expected to agree better with experimental data than do the SPDT prediction(eq. 3.4.1). This is seen in Fig. 5.11(the solid line). The values of the geometric factors 0.60 for n_{2c} and 0.80 for n_{1c} are found to best fit the theoretical prediction of the dielectric constant eq. 3.6.1 with experimental data taken from Furukawa *et al*² as shown in Fig. 5.12(the solid line) with a correlation coefficient of 0.99 which is significant at 0.001 α value. These values appear to be significantly different from those of the dielectric constant. The higher values of n_{1c} and n_{2c} implies that the inclusions are elongated and perpendicular to the applied stress. This is consistent with the predictions on geometry based on the dielectric constant.

5.3.1.3 THE PIEZOELECTRIC d CONSTANT

In this section, the theoretical prediction (eqs. 4.2.20-4.2.23 in 4.3.6) and the SPDT prediction (eqs. 4.2.12-4.2.19 in 4.3.6) for the piezoelectric d constant are tested on experimental data of a 0-3 connectivity composite. This is shown in Figure 5.12, which is a plot of the piezoelectric d constant versus the PZT volume fraction. In the figure, points are experimental data, the dashed line is the SPDT prediction (eqs. 4.2.12-4.2.19 in 4.3.6) and the solid line is the theoretical prediction (eqs. 4.2.20-4.2.23 in 4.3.6). The piezoelectric d constants of the pure PZT and polymer 184 and 0 pC/N, respectively, are used in the theoretical calculations.

We have seen in sections 2.4, 3.4 and 4.2 that the SPDT prediction does not involve shape parameter. In other words, the effect of shape of inclusions are ignored in the SPDT predictions. In addition, the model treats one component always as a solute and the other always as a solvent. As a result, the predictions of the SPDT are expected to be poor in the middle volume fraction range where there can be percolation. This is exactly what we see in Fig. 5.12 (the dashed line).

The theoretical prediction (eqs. 4.2.20-4.2.23 in 4.3.6) include the effect of shape of inclusions and at the same time the model treats both components symmetrically (there is a phase inversion at percolation threshold). As a result, the prediction is expected to agree better with experimental data than do the SPDT prediction. This is seen in Fig. 5.12 (the solid line). The values of the geometric factors 0.55 for n_{11} , 0.23 for

$n_{2\epsilon}$, 0.60 for $n_{2\sigma}$ and 0.80 for $n_{1\epsilon}$ are found to best fit the theoretical prediction eq. 4.2.20-4.2.23 in 4.3.6 with the experimental data taken from Furukawa *et al*² as shown in Fig. 5.13(the solid line) with a correlation coefficient of 0.99 which is significant at 0.001 α value. At first approximation, one expects those values of $n_{1\epsilon}$ and $n_{2\epsilon}$ which were used in the prediction of the dielectric constant(section 5.3.1.1) to be the same as those values of $n_{1\epsilon}$ and $n_{2\epsilon}$ used in the prediction of the piezoelectric d constant. The reason for their difference might be because those values of $n_{1\epsilon}$ and $n_{2\epsilon}$ used in section 5.3.1.1 are for 'stress-free' dielectric constant but those values of $n_{1\epsilon}$ and $n_{2\epsilon}$ used in this section are with stress. We expect the dielectric property of a composite to change when stress is applied to it.

5.3.2 TEST ON 0 - 3 CONNECTIVITY OF A COMPOSITE WHERE BOTH PHASES HAVE PIEZOELECTRIC ACTIVITY.

In this section, the theoretical predictions(eqs. 4.2.20-4.2.23 in 4.3.6) and the predictions of the spherical particles dispersion theory(SPDT)(eqs. 4.2.12-4.2.19 in 4.3.6) for the piezoelectric d constant of composite materials are tested with experimental data taken from Habtamu *et al*²⁰.

The composite system is a lead zirconate titanate(PZT)-polyvinylidene fluoride/ trifluoroethylene(PVDF/TrFE) system. The PZT powder is expected to have on the average spherical shape and to be homogeneously distributed in the polymer matrix. Here,

the piezoelectric activity comes from both the PZT and the polymer phases.

This is shown in Figure 5.13, which is a plot of the two predictions and the experimental data on the piezoelectric d constant versus the PZT volume fraction. In the figure, points are experimental data, the dashed line is the SPDT prediction (eqs. 4.2.12-4.2.19 in 4.3.6) and the solid line is the theoretical prediction (eqs. 4.2.20-4.2.23 in 4.3.6.). The piezoelectric d constants of the pure PZT and polymer 198 and -20 pC/N , respectively, are used in the theoretical calculations. The composite is expected to take intermediate values and to be dominated by the polymer phase.

As discussed in sections 2.4, 3.4, 4.2 and 5.3.1.3, the SPDT predictions are expected to be poor in the middle volume fraction range where there can be percolation. This is exactly what we see in Fig. 5.13 (the dashed line).

The theoretical prediction (eqs. 4.2.20-4.2.23 in 4.3.6) include the effect of shape of inclusions and at the same time the model treats both components symmetrically (there is a phase inversion at percolation threshold). As a result, the prediction is expected to agree better with experimental data than do the SPDT prediction. This is seen in Fig. 5.13 (the solid line). The values of the geometric factors 0.75 for n_{1c} , 0.49 for n_{2c} , 0.33 for n_{2c} and 0.33 for n_{1c} are found to best fit the theoretical prediction eq. 4.2.20-4.2.23 in 4.3.6 with the experimental data taken from Furukawa *et al*² as shown in Fig.

5.12(the solid line) with a correlation coefficient of 0.99 which is significant at 0.01 α value.

5.3.3 TEST ON COMPOSITE SYSTEMS WITH 1 - 1 AND 1 - 3 CONNECTIVITY.

In this section, the theoretical predictions(eqs. 2.5.7 for the dielectric constant and 4.2.20-4.2.23 in 4.3.6 for the piezoelectric d constant) and the predictions of the spherical particles dispersion theory(SPDT)(eqs. 2.4.9 for the dielectric constant and 4.2.12-4.2.19 in 4.3.6 for the piezoelectric d constant) are tested with experimental data taken from Habtamu et al²⁰.

The composite system is a lead zirconate titanate(PZT)-epoxy resin system. The 1-1 and 1-3 connectivity model is equivalent to the parallel model and the two components are expected to be prolate shaped.

5.3.3.1 THE PIEZOELECTRIC d CONSTANT

In this section, the theoretical prediction(eqs. 4.2.20-4.2.23 in 4.3.6) and the SPDT prediction(eqs. 4.2.12-4.2.19 in 4.3.6) for the piezoelectric d constant are tested on experimental data of a 1-1 and 1-3 connectivity composite. This is shown in Figure 5.14, which is a plot of the piezoelectric d constant versus the PZT volume fraction. In the figure, points are experimental data, the dashed line is the SPDT prediction(eqs. 4.2.12-4.2.19 in 4.3.6) and the solid line is the

theoretical prediction (eqs. 4.2.20-4.2.23 in 4.3.6.). The piezoelectric d constants of the pure PZT and polymer 390 and 0 pC/N, respectively, are used in the theoretical calculations. The composite is expected to take intermediate values and to be dominated by the PZT phase.

As discussed in the previous sections, the predictions of the SPDT are expected to be poor in the middle volume fraction range where there can be percolation. This is exactly what we see in Fig. 5.14 (the dashed line). This is because one component is always solute and the other is always solvent and as a result there is no phase inversion at percolation threshold.

The theoretical prediction (eqs. 4.2.20-4.2.23 in 4.3.6) include the effect of shape of inclusions and at the same time the model treats both components symmetrically (there is a phase inversion at percolation threshold). As a result, its prediction is expected to agree better with experimental data than do the SPDT prediction. This is seen in Fig. 5.14 (the solid line). The values of the geometric factors 0.89 for $n_{1\epsilon}$, 0.11 for $n_{2\epsilon}$, 0.99 for $n_{2\sigma}$ and 0.08 for $n_{1\sigma}$ are found to best fit the theoretical prediction eq. 4.2.20-4.2.23 in 4.3.6 with the experimental data taken from Habtamu *et al*²⁰ as shown in Fig. 5.14 (the solid line) with a correlation coefficient of 0.98 which is significant at 0.01 α value. The geometric factors used in eq. 4.2.20-4.2.23 are 0.89 for $n_{1\epsilon}$, 0.11 for $n_{2\epsilon}$, 0.99 for $n_{2\sigma}$ and 0.08 for $n_{1\sigma}$.

5.3.3.2 THE DIELECTRIC CONSTANT

Here, the theoretical prediction (eq. 2.5.7) and the SPDT prediction (eq. 2.4.9) for the dielectric constant are tested on experimental data of a 1-1 and 1-3 connectivity composite. This is shown in Figure 5.15, which is a plot of the dielectric constant ϵ versus the PZT volume fraction. In the figure, points are experimental data, the dashed line is the SPDT prediction (eq. 2.4.9) and the solid line is the theoretical prediction (eq. 2.5.7). The dielectric constants of the pure PZT and polymer 1540 and 3, respectively, are used in the theoretical calculations. The composite is expected to have intermediate values and to be dominated by the PZT phase.

As discussed in sections 2.4 and 5.3.1.1 the SPDT predictions does not involve shape parameter. In other words, the effect of shape of inclusions are ignored in the SPDT predictions. In addition, the model treats one component always as a solute and the other always as a solvent. As a result, the predictions of the SPDT are expected to be poor in the middle volume fraction range where there can be percolation. This is exactly what we see in Fig. 5.15 (the dashed line).

The theoretical prediction in section 2.5 (eq. 2.5.7) include the effect of shape of inclusions and at the same time the model treats both components symmetrically (there is a phase inversion at percolation threshold). As a result, the prediction by eq. 2.5.7 is expected to agree better with experimental data than do the SPDT prediction (eq. 2.4.9). This is seen in Fig. 5.15 (the

solid line). The values of the geometric factors 0.011 for n_2 and 0.0045 for n_1 , are found to best fit the theoretical prediction of the dielectric constant eq. 2.5.7 with experimental data taken from Habtamu et al² as shown in Fig. 5.15 (the solid line) with a correlation coefficient of 0.94 which is significant at 0.05 α value. This is consistent with our expectation that systems with 1-1 and 1-3 connectivity should fit nearly the parallel model (prolate-shaped inclusions and thus $n \approx 0$).

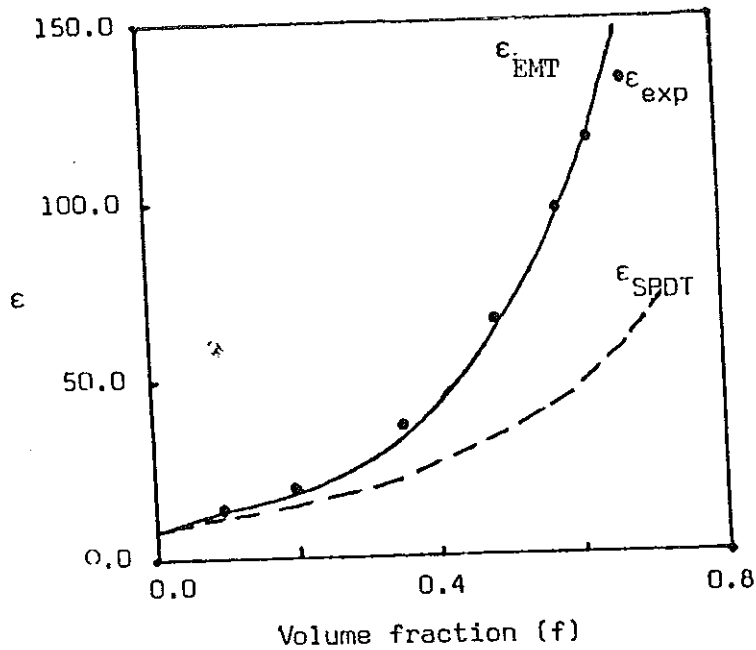


Fig. 5.10 PZT volume fraction dependence of the dielectric constant of a PZT-PVDF composite.

ϵ_{EMT} = theoretical prediction by EMT (eq. 2.5.7)

ϵ_{SPDT} = theoretical prediction by SPDT (eq. 2.4.9)

ϵ_{exp} = experimental data (dots)

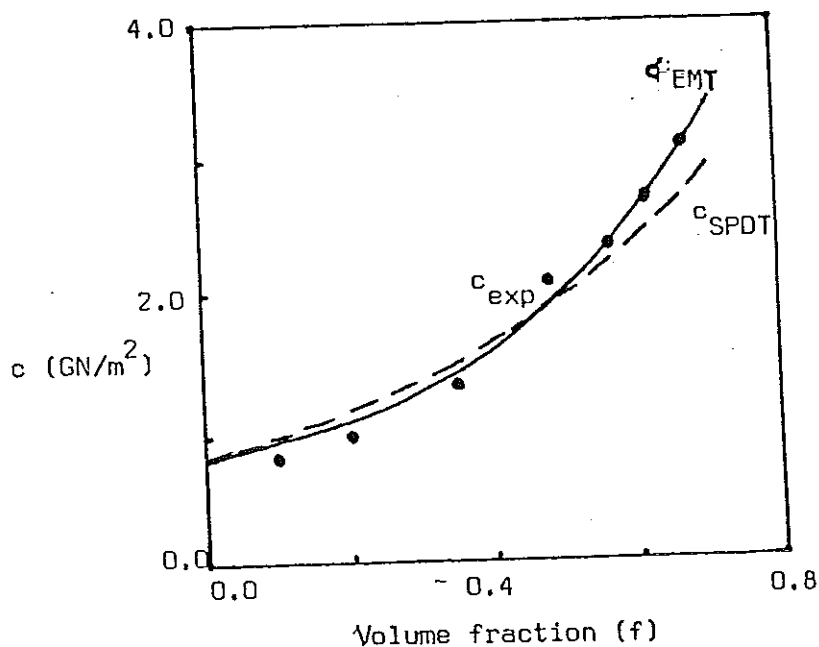


Fig. 5.11 PZT volume fraction dependence of the elastic constant of a PZT-PVDF composite.

c_{EMT} = theoretical prediction by EMT (eq. 3.6.1)

c_{SPDT} = theoretical prediction by SPDT (eq. 3.4.1)

c_{exp} = experimental data (dots)

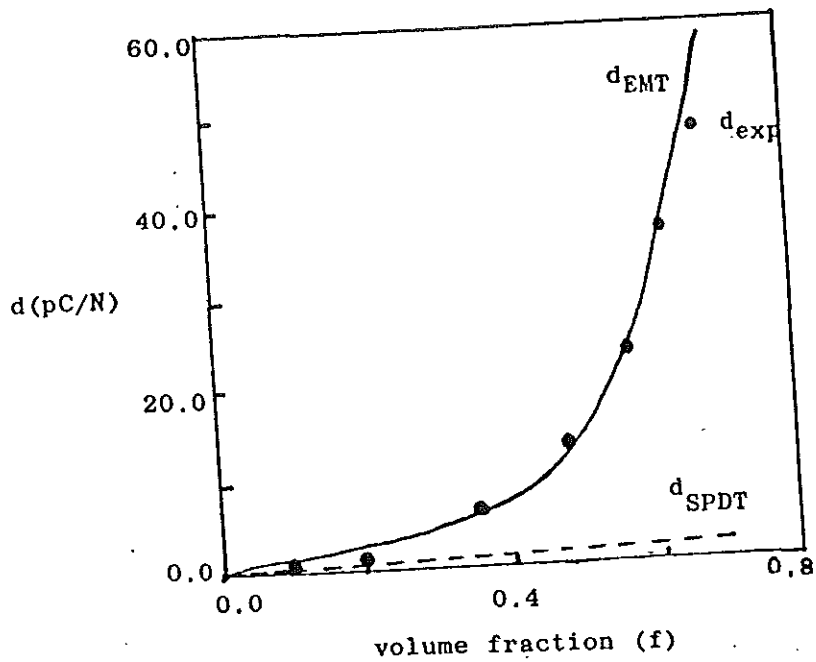


Fig. 5.12 PZT volume fraction dependence of the piezoelectric d constant of a PZT-PUDF composite.

d_{EMT} = theoretical prediction by EMT (eqs 4.2.20 - 4.2.23 in 4.3.6)

d_{SPDT} = theoretical prediction by SPDT (eqs 4.2.12 - 4.2.19 in 4.3.6)

d_{exp} = experimental data (dots)

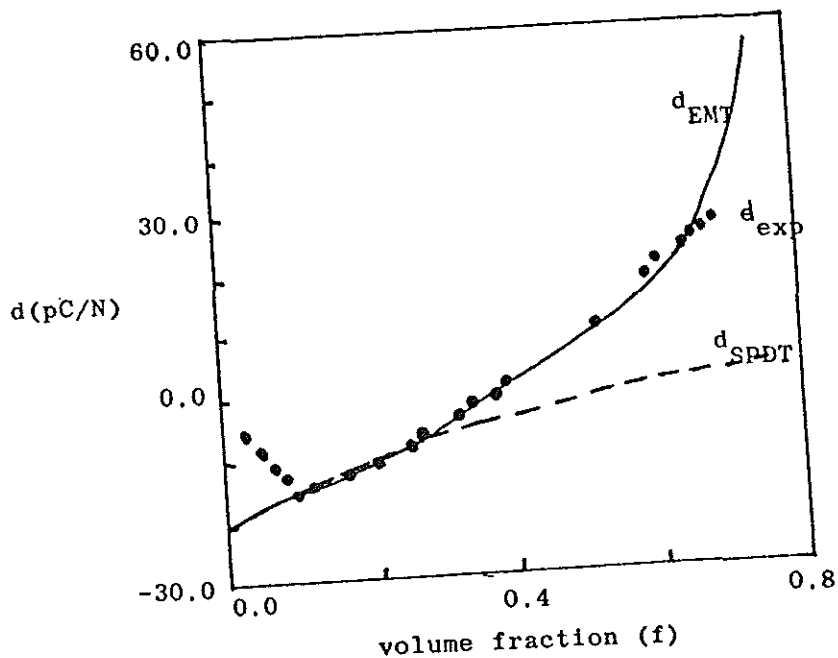


Fig. 5.13 PZT volume fraction dependence of the piezoelectric d constant of a PZT-VDF/TrFE composite

d_{EMT} = theoretical prediction by EMT (eqs 4.2.20 - 4.2.23 in 4.3.6)

d_{SPDT} = theoretical prediction by SPDT (eqs 4.2.12 - 4.2.19 in 4.3.6)

d_{exp} = experimental data (dots)

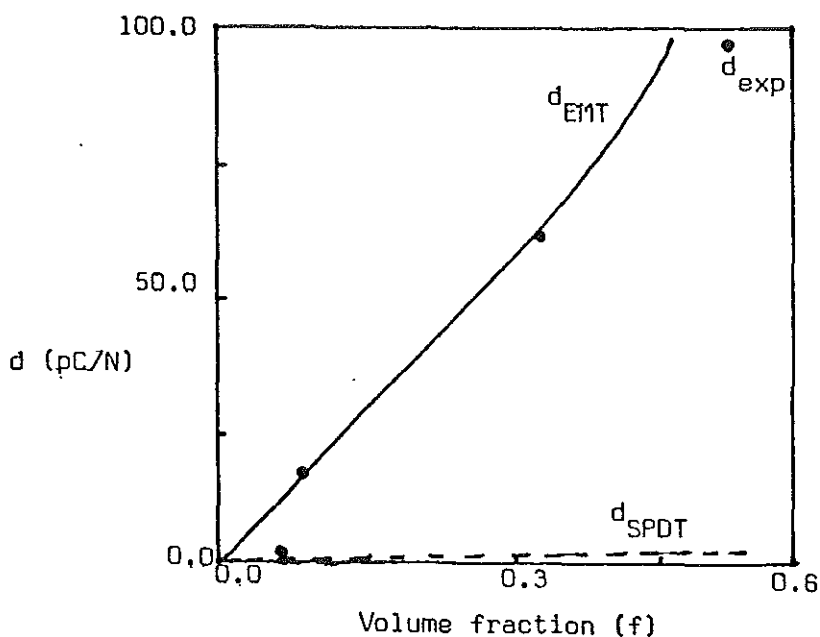


Fig. 5.14 PZT volume fraction dependence of the piezoelectric d constant of a PZT-EPOXY resin composite.

d_{EMT} = theoretical prediction by EMT (Eqs. 4.2, 20-4.2.23 in 4.3.6)

d_{SPDT} = theoretical prediction by SPDT (eqs. 4.2.12-4.2.19 in 4.3.6)

d_{exp} = experimental data (dots)

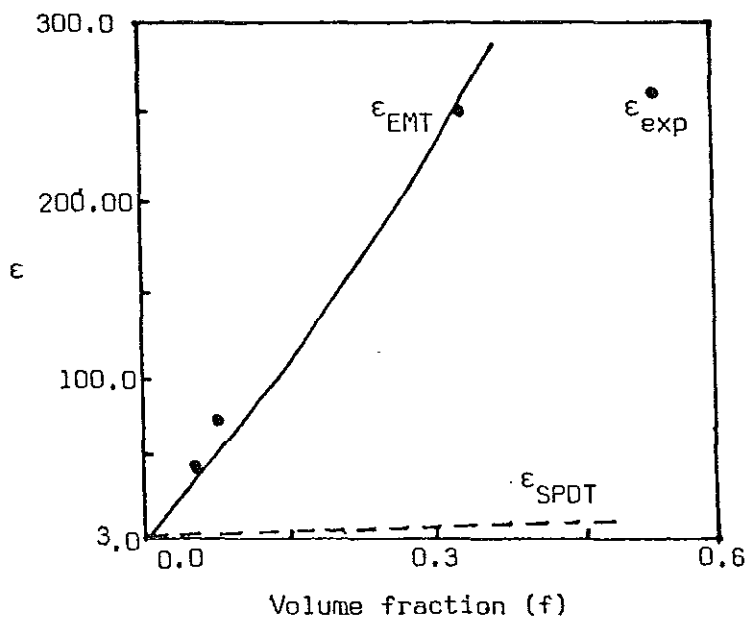


Fig. 5.15 PZT volume fraction dependence of the dielectric constant of a PZT-EPOXY resin composite.

ϵ_{EMT} = theoretical prediction by EMT (eq. 2.5.7)

ϵ_{SPDT} = theoretical prediction by SPDT (eq. 2.4.9)

ϵ_{exp} = experimental data (dots)

5.4 COMPARISON WITH EXPERIMENTAL DATA

(TEMPERATURE DEPENDENCE)

In section 5.3 we have tested the theoretical predictions with experimental data where we had plots of the properties versus PZT volume fraction. In this section, we will see if the theoretical predictions can be used to study the temperature dependence of the dielectric, elastic, and piezoelectric properties of composite materials.

In all the previous discussions we have treated the properties of the composites as real quantities. The dielectric, elastic, and the piezoelectric properties of composite materials depend on the temperature of measurement²⁵. The piezoelectric constants show relaxations where thermal relaxations in mechanical and dielectric properties take place. As a result, these constants are expressed as complex quantities for sinusoidal excitations of the form,

$$\epsilon = \epsilon' - j\epsilon'' \quad (5.4.1)$$

$$c = c' + jc'' \quad (5.4.2)$$

$$d = d' - jd'' \quad (5.4.3)$$

$$e = e' - je'' \quad (5.4.4)$$

$$g = g' - jg'' \quad (5.4.5)$$

$$h = h' - jh'' \quad (5.4.6)$$

To make things clear, let's first discuss a little about the complex properties of composites taking dielectric property as an example.

Consider a parallel plate capacitor which a capacitance C_0

in air and the space between the plates is filled by a medium of dielectric constant ϵ then, the capacitance becomes $C = \epsilon C_0$. When an alternating electromotive force V is applied across the capacitor an alternating current i will flow, its value being $i = j\omega\epsilon C_0 V$ provided that the dielectric is a 'perfect' one. In general, however, an in-phase component of current will appear corresponding to a resistive current between the parallel plates. Such current is entirely due to the dielectric medium and is a property of it. We therefore characterize it by a component of dielectric constant by defining relative dielectric constant as

$$\epsilon = \epsilon' - j\epsilon''.$$

The current in the capacitor then becomes

$$i = j\omega(\epsilon' - j\epsilon'')C_0V$$

or
$$i = \omega\epsilon''C_0V + j\omega\epsilon'C_0V$$

and has a real component. The magnitude of ϵ'' will be defined by the in-phase, or 'loss', component of the current. It is conventional to describe the performance of a capacitor in terms of its loss angle δ which is the phase angle between the total current i and the purely quadrature component i_0 . If the in-phase component is i_L , then

$$|i| = (|i_L|^2 + |i_0|^2)^{1/2}$$

and
$$\tan\delta = |i_L|/|i_0| = (\omega\epsilon''C_0V)/(\omega\epsilon'C_0V) = \epsilon''/\epsilon'$$

When the dielectric medium is 'loss-free', ϵ'' will be zero. ϵ'' is related to the dielectric conductivity σ_d as $\sigma_d = \omega\epsilon_0\epsilon''$. The dielectric conductivity σ_d represents the sum of all the loss mechanisms in the material, and is a measure of the performance

of a dielectric as an insulator.

Coming back to the point, the temperature dependence of the dielectric, elastic, and the piezoelectric properties of composite materials is studied by studying the temperature dependence of their loss tangents, $\tan\delta$, whose expressions are given below,

$$\tan\delta_\epsilon = \epsilon''/\epsilon' \quad (5.4.7)$$

$$\tan\delta_c = c''/c' \quad (5.4.8)$$

$$\tan\delta_d = d''/d' \quad (5.4.9)$$

$$\tan\delta_e = e''/e' \quad (5.4.10)$$

$$\tan\delta_g = g''/g' \quad (5.4.11)$$

$$\tan\delta_h = h''/h' \quad (5.4.12)$$

where ϵ is the dielectric constant, c is the elastic constant and d , e , g , h are the piezoelectric constants.

The theoretical predictions (eq. 2.5.7 for the dielectric constant, 3.6.1 for the elastic constant and eqs. 4.2.20-4.2.23 in 4.3.6-4.3.9 for the piezoelectric constants d , e , g , and h) and the predictions of the SPDT (eqs. 2.4.9 for the dielectric constant, 3.4.1 for the elastic constant and eqs. 4.2.12-4.2.19 in 4.3.6-4.3.9 for the piezoelectric constants d , e , g , and h) are generally valid at any temperature if the corresponding values of the single component constants are used. The geometric factors n_1 and n_2 representing the average shape of inclusions should work at any temperature.

The theoretical predictions (eqs. 2.5.7, 3.6.1, and 4.2.20-4.2.23 in 4.3.6-4.3.9) and the SPDT predictions (eqs. 2.4.9,

3.4.1, and 4.2.12-4.2.19 in 4.3.6-4.3.9) of the constants ϵ , c , d , e , g , and h of the composite materials are used to calculate the effective constants of the composite materials. These effective constants are then used in eqs. 5.4.7-5.4.12 to study the temperature dependence of the properties of composite materials. For example, ϵ'' and ϵ' of the composite material are evaluated using eq. 2.5.7 for the theoretical prediction and eq. 2.4.9 for the SPDT predictions where ϵ_2 and ϵ_1 are the dielectric constants of the pure phases, phase 2 and phase 1, at that specific temperature taken from Furukawa et al⁵. These values of ϵ'' and ϵ' are used in eq. 5.4.7 to calculate $\tan\delta$, at that specific temperature at a fixed PZT volume fraction f . This is repeated for the whole temperature range to be studied and is then compared with experimental data taken from Furukawa et al⁵ on the dielectric constant of the composite material measured at different temperatures. The same procedure is followed for the elastic and the piezoelectric constants. The study is done on a PZT-epoxy resin composite with $f= 0.131$.

The theoretical predictions (solid lines in Fig. 5.16-5.21) are in a relatively better agreement with experimental data than do the predictions of the spherical particles dispersion theory (SPDT) (dashed lines in Fig. 5.16-5.21). The values of the geometric factors which are found to best fit the theoretical prediction with the experimental data taken from Furukawa et al⁵ as shown in Figs. 5.16-5.21 are: n_{2e} is 0.05 for $\tan\delta_e$, and 0.10 for $\tan\delta_d$, $\tan\delta_s$, $\tan\delta_a$, and $\tan\delta_h$; n_{1e} is 0.25 for $\tan\delta_e$, and 0.15

for $\tan\delta_d$, $\tan\delta_e$, $\tan\delta_g$, and $\tan\delta_h$; n_{20} is 0.18 for $\tan\delta_c$, 0.02 for $\tan\delta_d$, $\tan\delta_e$, and $\tan\delta_h$, and 0.001 for $\tan\delta_g$; n_{10} is 0.10 for $\tan\delta_c$, $\tan\delta_e$, and $\tan\delta_g$, 0.05 for $\tan\delta_d$ and 0.15 for $\tan\delta_h$. The correlation coefficients are: 0.93 which is significant at 0.001 α value for $\text{Tan}\delta\epsilon$, 0.99 which is significant at 0.001 α value for $\text{Tan}\delta c$, 0.87 which is significant at 0.001 α value for $\text{Tan}\delta d$, 0.85 which is significant at 0.001 α value for $\text{Tan}\delta e$, 0.76 which is significant at 0.001 α value for $\text{Tan}\delta g$, and 0.90 which is significant at 0.001 α value for $\text{Tan}\delta h$.

The difference between the SPDT and the theoretical predictions is ascribed to the effect of shape of inclusions and to the symmetrical treatment of both components in the theoretical predictions. Thus the theoretical predictions are extended to the study of the temperature dependence of the properties of composite materials.

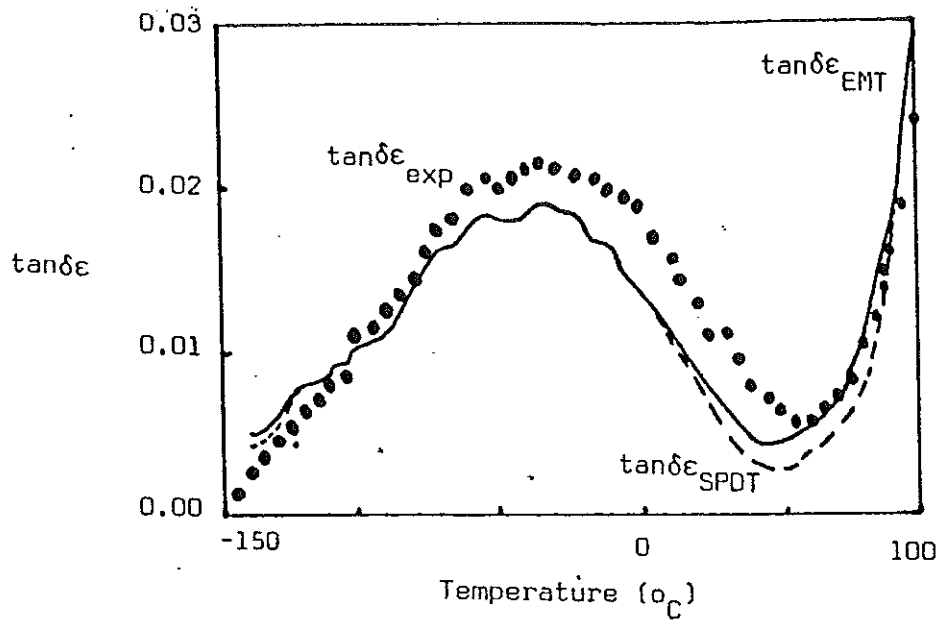


Fig. 5.16: Temperature dependence of $\tan\delta$ of the dielectric constant of a PZT-EPOXY resin system with $f = 0.131$.

$\tan\delta_{EMT}$ = theoretical prediction by EMT,

$\tan\delta_{SPDT}$ = theoretical prediction by SPDT,

$\tan\delta_{exp}$ = experimental data (dots),

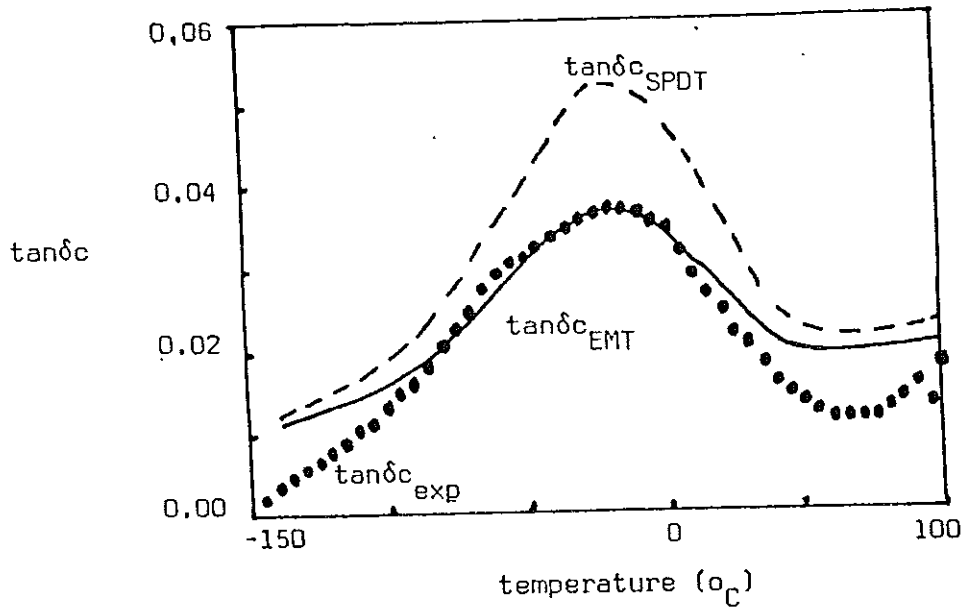


Fig. 5.17: Temperature dependence of $\tan\delta$ of the electric constant of a PZT-EPOXY resin system with $f = 0.131$.

$\tan\delta_{EMT}$ = theoretical prediction by EMT,

$\tan\delta_{SPDT}$ = theoretical prediction by SPDT,

$\tan\delta_{exp}$ = experimental data (dots).

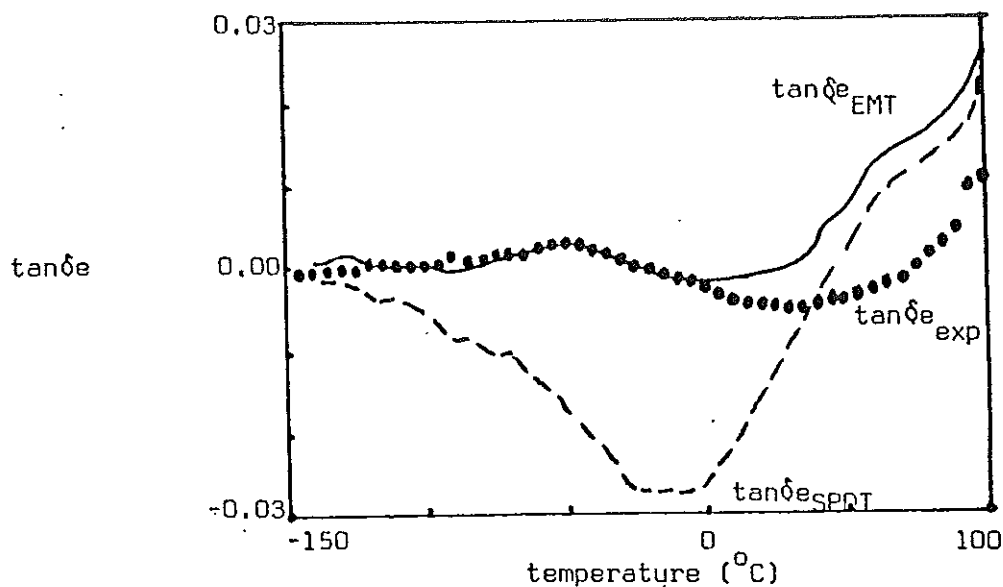


Fig. 5.18: Temperature dependence of $\tan\delta$ of the piezoelectric e constant of a PZT-EPOXY resin system with $f=0.131$.

$\tan\delta_{e_EMT}$ = theoretical prediction by EMT,
 $\tan\delta_{e_SPDT}$ = theoretical prediction by SPDT,
 $\tan\delta_{e_exp}$ = experimental data (dots).

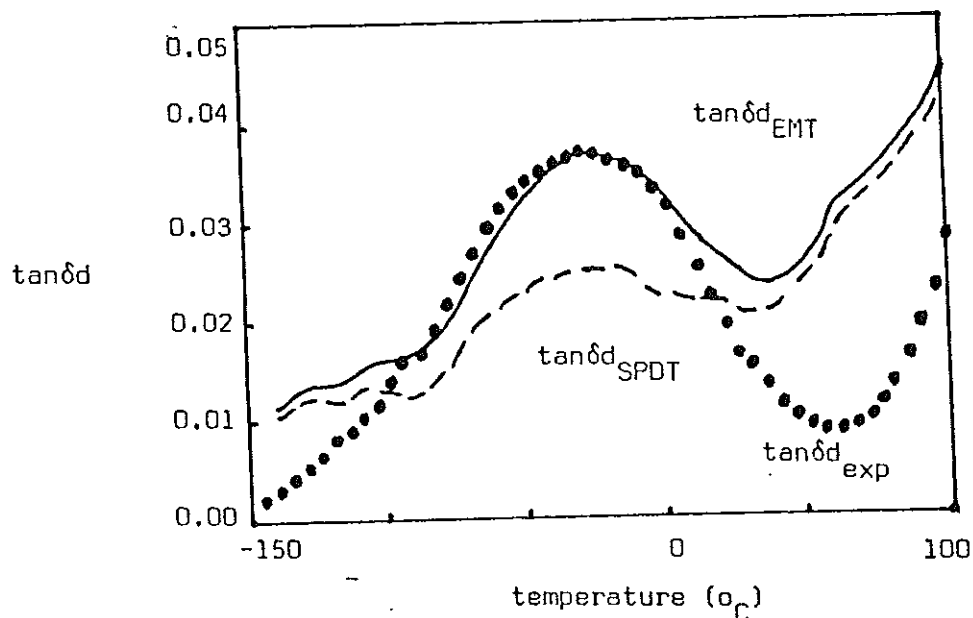


Fig. 5.19: Temperature dependence of $\tan\delta$ of the piezoelectric d constant of a PZT-EPOXY resin system with $f=0.131$.

$\tan\delta_{d_EMT}$ = theoretical prediction by EMT,
 $\tan\delta_{d_SPDT}$ = theoretical prediction by SPDT,
 $\tan\delta_{d_exp}$ = experimental data (dots).

7. REFERENCES

1. T. Furukawa, K. Suzuki, and M. Date, Ferroelectrics, 68, 33(1986).
2. T. Furukawa, K. Fujino, and E. Fukada, Japan J. Appl. Phys., 15, 2119(1979).
3. B. Jaffe, W. R. Cook, and H. Jaffe, Piezoelectric Ceramics, Academic Press, London(1971).
4. T. Yamada, T. Ueda, and T. Kitayama, J. Appl. Phys., 53, 4328(1982).
5. T. Furukawa, K. Ishida, and E. Fukada, Japan Appl. Phys., 50, 4904(1976).
6. K. Torii, T. Kaga, K. Kushida, H. Takeueshi, and E. Takeda, Jap. J. Appl. Phys., 30, 3562(1991).
7. T. R. Shrout, L. J. Bowen, and W. A. Schulze, Mater. Res. Bull., 15, 1371(1980).
8. R. E. Newnham, D. P. Skinner, K. A. Klicker, A. S. Bhalla, B. Hardiman, and T. R. Gururaja, Ferroelectrics, 2, 49(1980).
9. L. J. Bowen and T. R. Gururaja, J. Appl Phys., 51, 5661(1980).
10. K. Lal and R. Parshad, J. Phys. D, 6, 1363(1973).
11. T. Furukawa, Phase Transitions, 18, 143(1989).
12. R. E. Newnham, Ferroelectrics, 68, 1(1986).
13. Y. T. Chen, J. Polym. Sci., 11, 2013(1973).
14. M. Date, Polymer J., 8, 60(1975).

15. L. Pardo, J. Mendiola, and C. Alemany, J. Appl. Phys., 64, 5092(1988).
16. L. Pardo, J. Mendiola, and C. Alemany, Ferroelectrics, 93, 183(1989).
17. N. Kawai and K. Fukuyama, J. Chem. Soc. Japan, 10, 129(1985).
18. F. Brouers, J. Phys. D, 19, 7183(1986).
19. W.T. Doyle and I.S. Jacobs, J. Appl. Phys., 71, 3926(1992).
20. Habtamu Zewdie and F. Brouers, J. Appl. Phys., 68, 713(1990).
21. L. D. Landau and E. M. Lifshitz, Electrodynamics of continuous media, Pergammon Press, London(1960).
22. W. R. Tinga, W. A. G. Voss and D. F. Blossey, J. Appl. Phys., 44, 3897(1973).
23. J. C. Anderson, Dielectrics, Chapman and Hall ltd. , London(1964).
24. E. Fatuzzo and W. J. Merz, Ferroelectricity, North - Holland Publishing Company, Amsterdam(1952).
25. C. J. F. Bottcher, Theory of electric polarisation, Elsevier Publishing Company, Amsterdam(1952).
26. T. Furukawa, IEEE Transaction on Electrical Insulation, 24, 375(1989).
27. S. P. Timoshenko and J. N. Goodier, Theory of Elasticity, 3rd ed. , McGraw - Hill, New York(1982)
28. Z. Hashin, Appl. Mech. Rev., 17, 1(1964).
29. E. Fukada and M. Date, Polymer J., 1(4), 410(1970).

30. D.A.G. Bruggeman, Ann. Phys., Lpz., 24, 636(1935).
31. K. W. Waggner, Arch. Electrotech., 2, 371(1914).

DECLARATION

I, the undersigned, declare that this thesis is my work and that all sources of material used for this thesis have been dully acknowledged.

Name: Hussen Mohammed

Signature: *Hussen M.*

Place and Date of submission: Chemistry Department
Addis Ababa University
March 6, 1994.

DECLARATION

I, the undersigned, declare that this thesis is my work and that all sources of material used for this thesis have been dully acknowledged.

Name: Hussen Mohammed

Signature: *Hussen M.*

Place and Date of submission: Chemistry Department
Addis Ababa University
March 6, 1994.

30. D.A.G. Bruggeman, Ann. Phys., Lpz., 24, 636(1935).
31. K. W. Wagner, Arch. Electrotech., 2, 371(1914).

15. L. Pardo, J. Mendiola, and C. Alemany, J. Appl. Phys., 64, 5092(1988).
16. L. Pardo, J. Mendiola, and C. Alemany, Ferroelectrics, 93, 183(1989).
17. N. Kawai and K. Fukuyama, J. Chem. Soc. Japan, 10, 129(1985).
18. F. Brouers, J. Phys. D, 19, 7183(1986).
19. W.T. Doyle and I.S. Jacobs, J. Appl. Phys., 71, 3926(1992).
20. Habtamu Zewdie and F. Brouers, J. Appl. Phys., 68, 713(1990).
21. L. D. Landau and E. M. Lifshitz, Electrodynamics of continuous media, Pergammon Press, London(1960).
22. W. R. Tinga, W. A. G. Voss and D. F. Blossey, J. Appl. Phys., 44, 3897(1973).
23. J. C. Anderson, Dielectrics, Chapman and Hall ltd. , London(1964).
24. E. Fatuzzo and W. J. Merz, Ferroelectricity, North - Holland Publishing Company, Amsterdam(1952).
25. C. J. F. Bottcher, Theory of electric polarisation, Elsevier Publishing Company, Amsterdam(1952).
26. T. Furukawa, IEEE Transaction on Electrical Insulation, 24, 375(1989).
27. S. P. Timoshenko and J. N. Goodier, Theory of Elasticity, 3rd ed. , McGraw - Hill, New York(1982)
28. Z. Hashin, Appl. Mech. Rev., 17, 1(1964).
29. E. Fukada and M. Date, Polymer J., 1(4), 410(1970).